NASA TECHNICAL NOTE

NASA TN D-5890

NASA TN D-5890

EVALUATION OF THE EFFECT OF A YAW-RATE DAMPER ON THE FLYING QUALITIES OF A LIGHT TWIN-ENGINE AIRPLANE

by Calvin R. Jarvis, Paul C. Loschke, and Einar K. Enevoldson

Flight Research Center
Edwards, Calif. 93523

NATIONAL AERONAUTICS AND SPACE ADMINISTRATION • WASHINGTON, D. C. • JULY 1970

1. Report No.	2. Government Accession No.	3. Recipient's Catalog No.
NASA TN D-5890		

4. Title and Subtitle	5. Report Date
EVALUATION OF THE EFFECT OF A YAW-RATE DAMPER ON THE FLYING QUALITIES OF A LIGHT TWIN-ENGINE AIRPLANE	July 1970
	6. Performing Organization Code

7. Author(s)	8. Performing Organization Report No.
Calvin R. Jarvis, Paul C. Loschke, and Einar K. Enevoldson	H-584

9. Performing Organization Name and Address	10. Work Unit No.
NASA Flight Research Center P.O. Box 273 Edwards, California 93523	125-19-01-03-24
	11. Contract or Grant No.

12. Sponsoring Agency Name and Address	13. Type of Report and Period Covered
National Aeronautics and Space Administration Washington, D. C. 20546	Technical Note
	14. Sponsoring Agency Code

15. Supplementary Notes

16. Abstract

A flight-test program was conducted with a light twin-engine airplane to determine the effect of a parallel yaw damper and aileron-to-rudder interconnect on the flying qualities of this class of aircraft. Both quantitative and qualitative results are presented for several flight tasks and conditions, including flight in turbulence. Airplane handling qualities and ride qualities are summarized. The effect of the yaw damper on the stall and post-stall motions of the test airplane and the motions resulting from sudden engine failure are also discussed.

17. Key Words (Suggested by Author(s))	18. Distribution Statement
Yaw damper General-aviation aircraft ILS landings	Unclassified - Unlimited

19. Security Classif. (of this report)	20. Security Classif. (of this page)	21. No. of Pages	22. Price*
Unclassified	Unclassified	46	$3.00

*For sale by the Clearinghouse for Federal Scientific and Technical Information
Springfield, Virginia 22151

EVALUATION OF THE EFFECT OF A YAW-RATE DAMPER ON THE FLYING QUALITIES OF A LIGHT TWIN-ENGINE AIRPLANE

By Calvin R. Jarvis, Paul C. Loschke, and
Einar K. Enevoldson
Flight Research Center

SUMMARY

A simple, parallel yaw damper and aileron-to-rudder interconnect was tested in flight in a light twin-engine airplane to evaluate the improvement that might be achieved in the overall flying qualities of a general-aviation airplane in turbulence. Fifteen pilots participated in the evaluation program. Both quantitative and qualitative data were obtained for evaluation of lateral-directional characteristics.

The yaw damper significantly reduced the short-period lateral-directional motions of the test airplane in turbulent air. This resulted in an improvement in both the ride and the flying qualities. The improvement in the pilot's overall performance of the ILS approach task was not significant.

The aileron-to-rudder interconnect was found to be effective in compensating for adverse aileron yaw, and turns could be made easier and more accurately.

An increase in the intensity of the lateral motions of the test airplane in turbulence was experienced when the autopilot system was used alone. The autopilot performance in turbulence was significantly improved when the system was used with the yaw damper.

Maximum roll and yaw rates encountered during stall maneuvers were reduced when the yaw damper was operating. Also, the available time for corrective action following a simulated engine failure was effectively doubled when the yaw damper was engaged.

INTRODUCTION

The NASA Flight Research Center recently conducted a handling-qualities survey (ref. 1) of a representative cross section of general-aviation aircraft. This study indicated that personal-owner aircraft have generally satisfactory handling qualities for visual flight and for instrument flight in smooth air, but that atmospheric turbulence degrades these handling qualities. The degradation was most noticeable during ILS approaches because of the marked increase in pilot workload. Low lateral stability, high adverse yaw, and objectionable Dutch roll characteristics are identified in references 1 and 2 as some of the stability and control characteristics which degraded

handling qualities. These characteristics, and others, combined to make precise instrument tracking tasks in turbulence difficult for even the most experienced instrument pilots.

In high-performance airplanes, lateral-directional-stability problems have been alleviated and often eliminated through the use of yaw dampers. Also, autopilot performance has been improved somewhat by including inner loops to optimize the rate of change in the attitudes controlled by the autopilot. The use of a yaw damper as a solution to similar general-aviation problems was believed to be both feasible and practical. Also, it was felt necessary to compensate for adverse-yaw effects and to provide automatic turn coordination by the incorporation of a system such as a filtered aileron-rudder interconnect. Therefore, the Flight Research Center installed a simple yaw-rate damper and an aileron-rudder interconnect in a light twin-engine airplane in parallel with the pilot's rudder-control system. A flight-test program was conducted, and the flying qualities of the airplane were evaluated. The results of the program are summarized in this report.

SYMBOLS

a_y	lateral acceleration, g or ft/sec^2
B	effective bandwidth, cps
B_s	analyzer bandwidth, cps
b	wing span, ft
$C_{h_{\delta_r}}$	rudder hinge-moment parameter, per deg
$C_{n_{\delta_r}}$	rudder-effectiveness parameter, per deg
$\bar{c}_r$	rudder mean aerodynamic chord, ft
f	frequency, cps
f_e	effective frequency, cps
G(s)	forward-loop transfer function
g	gravitational constant, 32 ft/sec^2
HM_{δ_r}	rudder hinge moment due to rudder deflection, in-lb/deg
H(s)	feedback-loop transfer function

I_X	moment of inertia about pitch axis, slug-ft^2
I_Y	moment of inertia about roll axis, slug-ft^2
I_Z	moment of inertia about yaw axis, slug-ft^2
$j = \sqrt{-1}$	
K_{amp}	amplifier gain, volt-sec/volt
$K_{constant}$	constant coefficient
K_D	damper gain, in-lb-sec/deg/sec
K_{gyro}	rate-gyro gain, volts/deg/sec
K_{OL}	open-loop gain, radians^{-1}
$K_{power\ amp}$	power-amplifier gain, mA/volt
K_{servo}	servoactuator gain, in-lb/mA
L_p	rolling acceleration due to roll rate, sec^{-1}
L_r	rolling acceleration due to yaw rate, sec^{-1}
L_β	rolling acceleration due to sideslip, sec^{-2}
L_{δ_a}	rolling acceleration due to aileron deflection, sec^{-2}
N_p	yawing acceleration due to roll rate, sec^{-1}
N_r	yawing acceleration due to yaw rate, sec^{-1}
N_β	yawing acceleration due to sideslip, sec^{-2}
N_{δ_a}	yawing acceleration due to aileron deflection, sec^{-2}
N_{δ_r}	yawing acceleration due to rudder deflection, sec^{-2}
n	statistical degrees of freedom

p	roll rate, deg/sec
$\dot{p}$	rolling acceleration, deg/sec^2
q	dynamic pressure, lb/ft^2
r	yaw rate, deg/sec
$\dot{r}$	yawing acceleration, deg/sec^2
S	wing surface area, ft^2
S_P	playback speed, IPS
S_R	recording speed, IPS
S_r	rudder surface area, ft^2
s	Laplace transform variable
T	data-tape length, sec
t	time, sec
V	airplane velocity, ft/sec
V_e	equivalent airspeed, ft/sec
V_i	indicated airspeed, knots
Y_p	side force due to roll rate, radians^{-1}
Y_r	side force due to yaw rate, radians^{-1}
Y_β	side force due to sideslip, sec^{-1}
Y_{δ_r}	side force due to rudder deflection, sec^{-1}
β	angle of sideslip, deg
$\dot{\beta}$	rate of change of sideslip, deg/sec
δ_a	total aileron deflection, deg
δ_f	wing-flap deflection, deg

δ_r	rudder deflection, deg
ζ	damping ratio
Φ_K	power spectral density of a function K
φ	bank angle, deg
ψ	aircraft heading angle, deg
$\Delta\psi$	change in aircraft heading, deg
ω	frequency, radians/sec
ω_d	damped natural frequency, radians/sec
ω_n	natural frequency, radians/sec

VEHICLE AND SYSTEM DESCRIPTION

Test Airplane

The airplane used for the flight-test program was a conventional, light twin-engine, low-wing monoplane. Physical characteristics of the airplane are presented in table 1. Control about each axis was conventional. The longitudinal-control surface was an all-movable horizontal stabilator with a geared anti-servo tab and with a deflection range from 4° trailing edge down to 14° trailing edge up. The control deflection of each aileron surface was 14° down to 18° up, and the rudder deflection was ±27°. A spring in the rudder system provided positive centering and trim of the rudder surface.

The airplane was equipped with a typical general-aviation autopilot and instrument landing system.

Yaw Damper

The test yaw damper used a fixed relationship between airplane yaw rate and applied rudder-control torque or hinge moment to change the rudder deflection. The hinge-moment-system concept is particularly attractive for use in general-aviation type of aircraft because it is considerably less complicated than position feedback. The technique also provides better closed-loop performance over a larger area of the flight envelope for fixed-gain operation, inasmuch as the surface deflection for a given yaw rate automatically increases or decreases with dynamic pressure to provide the required hinge moment.

The yaw-damper hardware consisted of three basic components: (1) an electromechanical servoactuator; (2) a rate gyro; and (3) an electronics assembly. A photograph of these components is shown in figure 1. A block diagram of the yaw damper

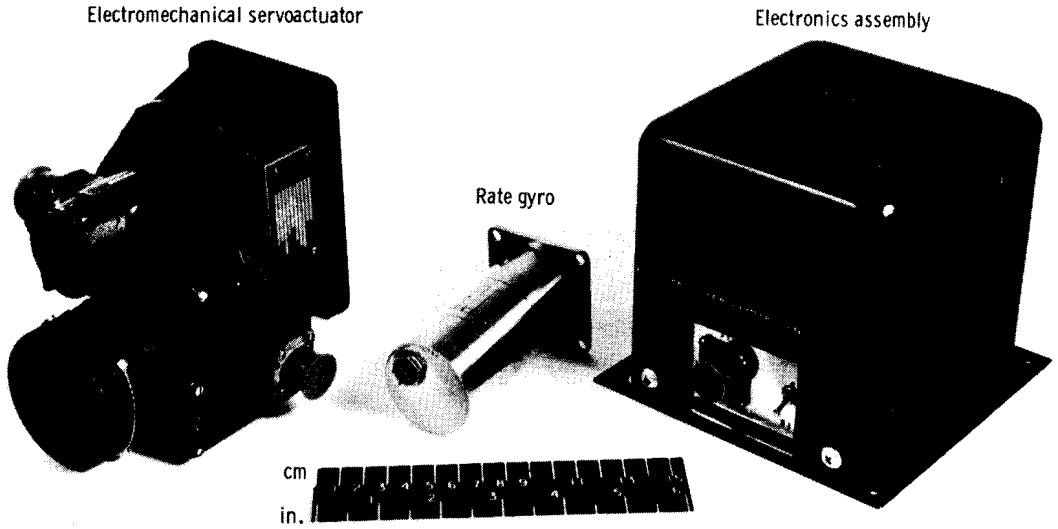

E-19402

Figure 1. Test airplane yaw-damper components.

is shown in figure 2, along with a schematic illustration showing the parallel connection of the damper actuator to the airplane rudder cabling. As a result of this parallel connection, actuator motion resulted in rudder-pedal motions. The clutch, an integral part of the servo capstan, was engaged only when the yaw damper was operating, and was set to slip for an applied torque of 200 in-lb, which corresponded to approximately

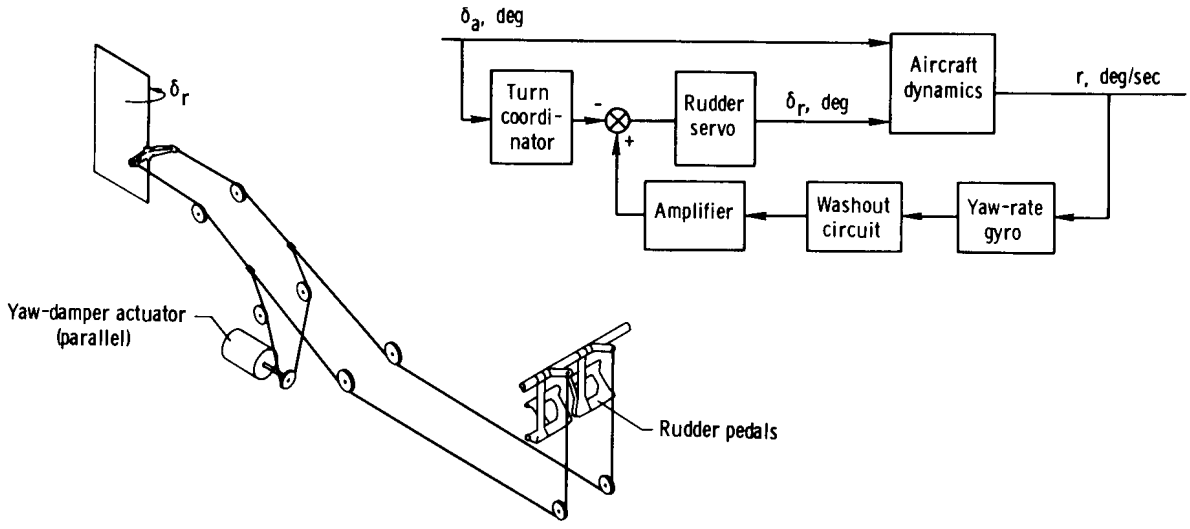

Figure 2. Block diagram of yaw damper and schematic drawing of parallel actuator installation in test airplane.

15 pounds of rudder-pedal force. The system could, therefore, be overridden by the pilot at any time.

Automatic turn coordination was achieved by using an electrical aileron-to-rudder interconnect. An electrical signal proportional to aileron deflection was appropriately shaped and applied to the rudder actuator. By proper selection of the shaping network, the rudder motion obtained in this manner could be used to compensate for aileron-induced yawing motions. Unless otherwise stated, the interconnect was utilized whenever the yaw damper was engaged.

Figure 3 shows the transfer-function block diagram of the system with the final gain values. The final values of electronic gain for the yaw damper and aileron-to-rudder interconnect were determined in flight. The electronics assembly also included a washout network with a time constant of 1 second, which was incorporated to eliminate the response of the actuator to steady-state yaw rates during constant turns.

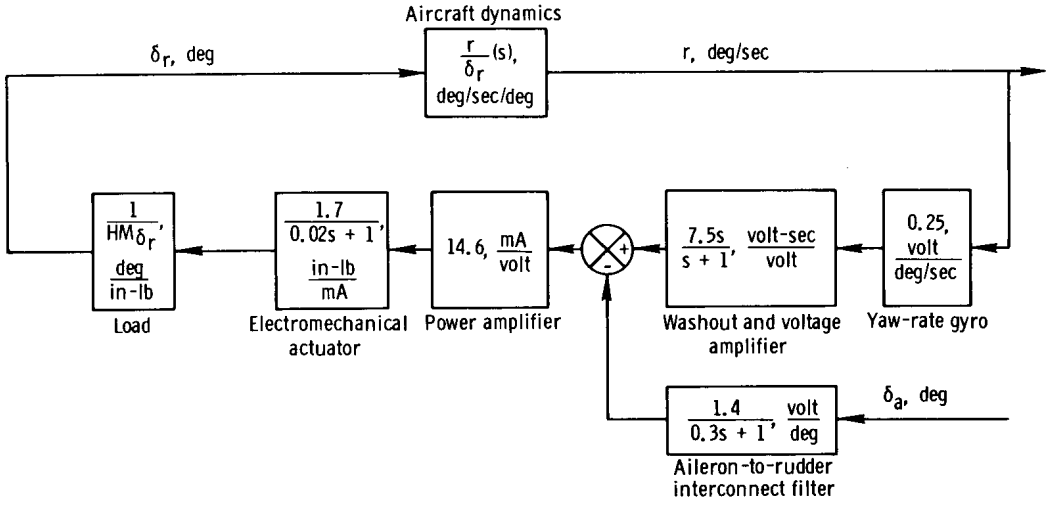

Figure 3. Block diagram of yaw damper and aileron-to-rudder interconnect.

The normalized frequency response of the yaw-damper system from gyro to rudder surface position is shown in figure 4. The second-order peaking at about 3 cps is

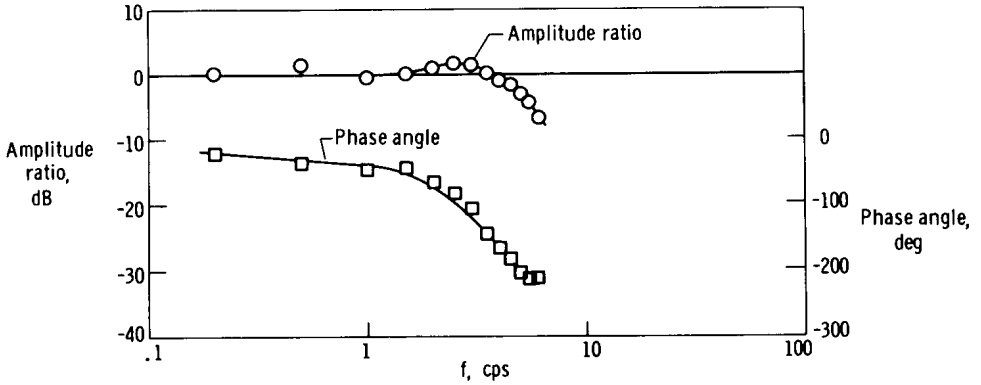

Figure 4. Frequency response of yaw damper from gyro to rudder position (unloaded).

accounted for by the spring bungee, which is part of the airplane's basic control system and is attached to the rudder surface to provide centering and trim.

The design of the yaw damper is discussed in more detail in appendix A. The airplane transfer functions used in establishing the design gains are presented in appendix B.

Autopilot System

The commercial autopilot used in the test airplane incorporated (in the lateral-directional axes) wings-leveler and heading-hold modes and controlled aileron position only. The system consisted of an electronic amplifier assembly, electromechanical actuator (200 in-lb), vacuum-powered vertical and directional gyros, and control panel. A block diagram of the lateral axis of the autopilot system is presented in figure 5.

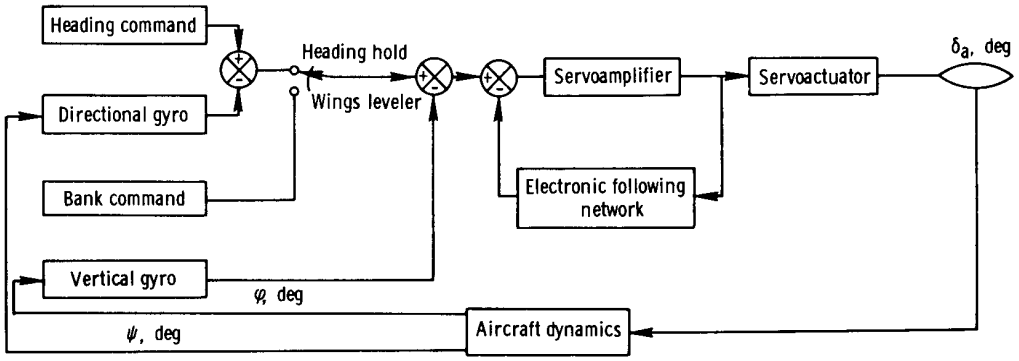

Figure 5. Simplified block diagram of the lateral axis of the test airplane autopilot.

In figure 6 the normalized frequency-response characteristics of the autopilot system are shown. The open-loop response (command-to-surface position) was essentially

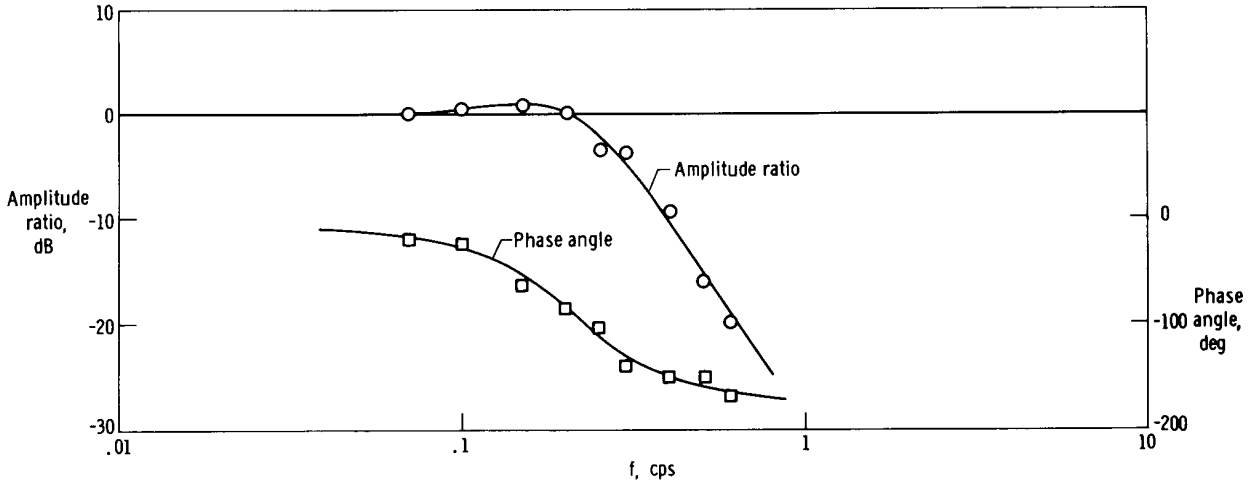

Figure 6. Frequency response of test airplane autopilot from gyro to servo position.

second order, with a bandwidth of approximately 0.2 cps and a damping ratio on the order of 0.5 with the servo essentially unloaded.

INSTRUMENTATION

A pulse code modulated (PCM) digital data-acquisition system was used during the flight-test program. Data were recorded onboard the airplane and by telemetry at a ground station. The recorded parameters and their ranges, sensitivities, and maximum frequency limits were as follows:

Parameter	Range	Sensitivity	Frequency, cps
Altitude	10,000 ft	50 ft	40
Airspeed	250 knots	3 knots	40
Right-hand aileron position	-19° to 15°	0.2°	40
Left-hand aileron position	-19° to 15°	0.2°	40
Rudder position	±24°	0.2°	40
Angle of sideslip	±20°	0.2°	40
Lateral acceleration	±0.25 g	0.005 g	10
Normal acceleration	0 to 4 g	0.02 g	10
Roll rate	±60 deg/sec	0.6 deg/sec	10
Yaw rate	±20 deg/sec	0.2 deg/sec	10
Roll acceleration	±4 radians/sec^2	0.04 radian/sec^2	40
Yaw acceleration	±2 radians/sec^2	0.02 radian/sec^2	40
Pedal force	±120 lb	1.5 lb	10
Wheel force	±80 lb	0.8 lb	10
Rudder hinge moment	±300 in-lb	1.2 in-lb	10
ILS glide-slope error	±0.5°	0.02°	40
ILS localizer error	±2.5°	0.1°	40

RESULTS AND DISCUSSION

Effect on Flying Qualities

Dutch roll characteristics. – During the first phase of the flight-test program, the effect of the yaw damper on the Dutch roll motions of the test airplane was determined. Rudder pulses were performed at several flight conditions with the airplane in the cruise and the approach configurations and with the yaw damper alternately engaged and disengaged.

The Dutch roll damping is shown in figure 7 as a function of velocity for the cruise configuration of the test airplane. The damping of the basic airplane is essentially constant at a damping ratio of 0.1 over the speed range of approximately 70 knots to 140 knots. With the yaw damper on, the Dutch roll damping is approximately 0.7 between 80 knots and 120 knots, and then increases at speeds greater than 120 knots.

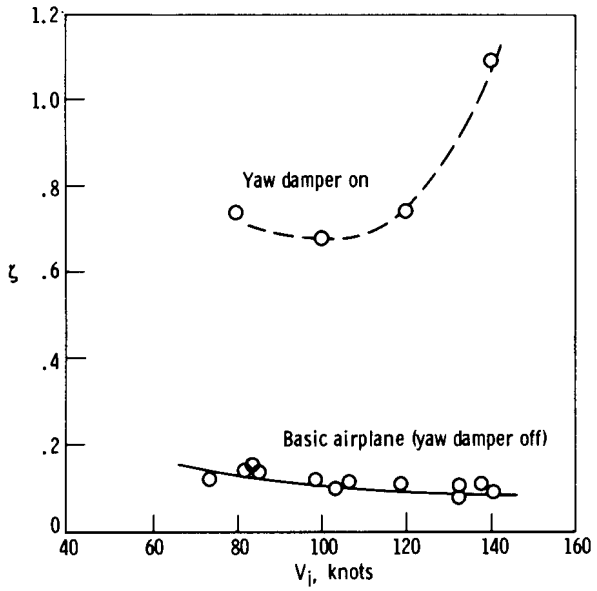

Figure 7. Variation of test airplane Dutch roll damping with velocity. Cruise configuration; altitude, 6000 ft.

The effect of the yaw damper on the test airplane motions during cruising flight in moderate turbulence is illustrated by the time history in figure 8. The yaw-rate

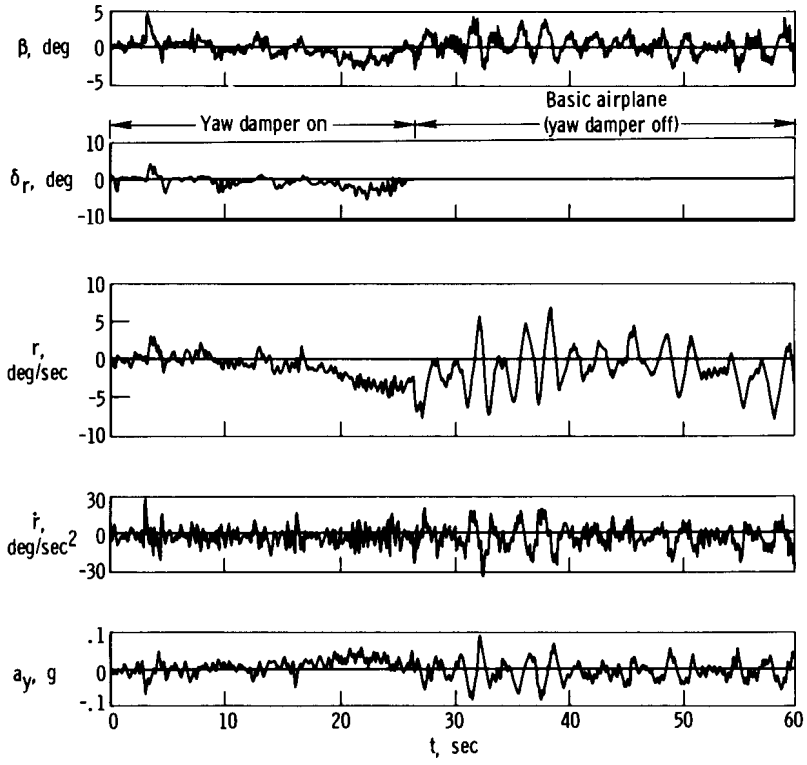

Figure 8. Test airplane response in moderate turbulence with and without yaw damper. Cruise configuration; V_i = 140 knots.

and sideslip traces show the effectiveness of the yaw damper in reducing the short-period Dutch roll motion excited by the turbulence. During the damper-on portion of the time history, the Dutch roll motions of these parameters are virtually eliminated. This was apparent to the pilot as an improvement, even though the sideslip and lateral-acceleration motions were increased at the lower frequencies with the yaw damper on. The effect, as seen by the pilots, was an increase in the lateral-directional rigidity of the airplane in turbulence.

A quantitative comparison of the reduced motions is shown in figure 9. This figure presents the power spectra of four lateral-directional parameters and compares the damper-on and damper-off operation. The power spectra were computed by using the technique described in appendix C. The frequency of the Dutch roll motion for the test airplane is apparent from the peaks that occur in the basic airplane power spectra at approximately 0.5 cps. The yaw damper significantly reduces the Dutch roll motion of the airplane, as is indicated by the much lower peaks of the yaw rate, sideslip, and lateral-acceleration power spectra for the damper-on configuration than for the damper-off configuration. Figure 9 also shows, for the damper-on configuration, a large increase in sideslip motions and lateral acceleration at the lower frequencies. This is attributed to the fact (discussed in ref. 3) that the yawing motion of an aircraft, at lower frequencies, is effective in alleviating sideslip resulting from side gusts. The yaw damper tends to eliminate this effect by reducing the aircraft yawing rates. Consequently, the aircraft has less tendency to oscillate in turbulence as a result of the changing relative wind vector. This increase in low-frequency sideslip motions was not apparent to the evaluation pilots, however, and tended to be masked by the reduction in the short-period motions. For maneuvering flight in the cruise configuration, the average pilot rating for the basic airplane was changed from marginally satisfactory to satisfactory-to-good by use of the yaw damper.

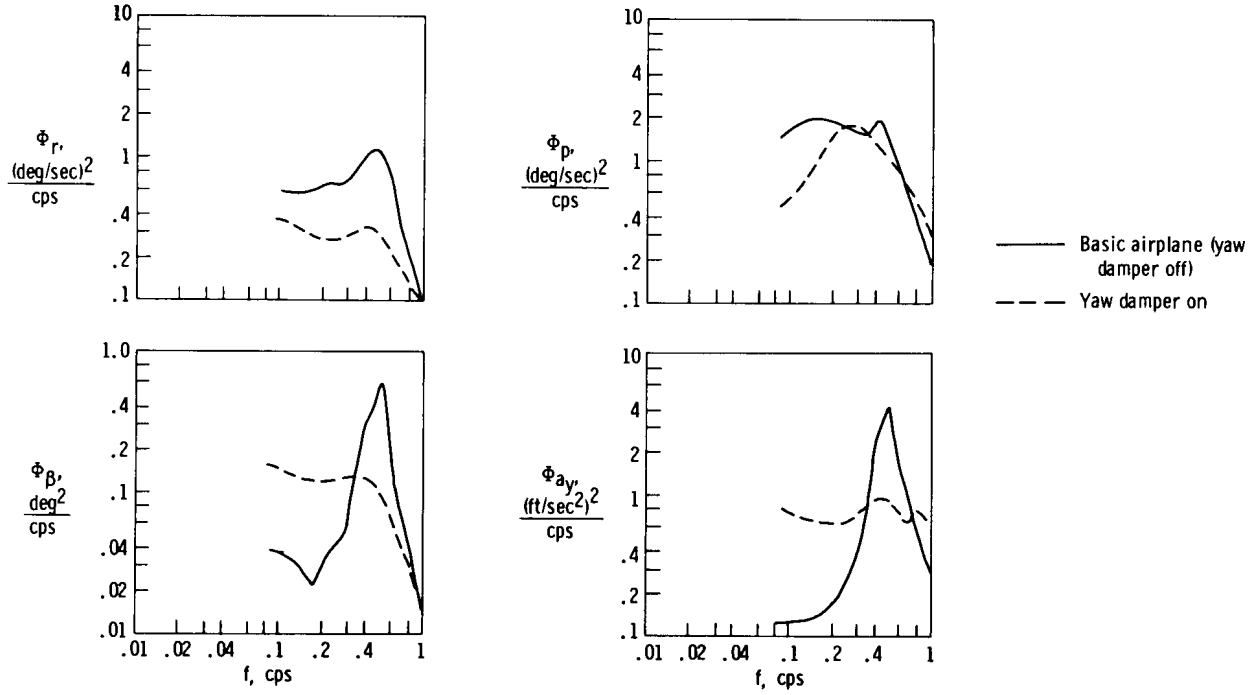

Figure 9. Flight-test results showing the comparison of airplane power spectra with and without the yaw damper for the cruise configuration in moderate turbulence. V_i = 140 knots; n = 60.

The effect of the yaw damper on airplane motions in moderate turbulence with the airplane in the approach configuration and flying at an airspeed of 80 knots is shown by the power spectra presented in figure 10. The frequency of the basic airplane short-period peaks has been reduced to 0.3 cps. The peaks are also considerably higher than those in figure 9, indicating more Dutch roll motions for this configuration than were experienced in the cruise configuration. The larger power losses (higher peaks) at the approach short-period frequencies are indicative of the decreased stability in turbulence at lower velocities which was associated with this class of aircraft (ref. 1). The effect of the yaw damper for the approach configuration is virtually identical to that for the cruise configuration. It should be noted, however, that the improvement afforded by the damper is much more apparent in the approach than in cruising flight because of the poorer stability characteristics of the test airplane at slower airspeeds.

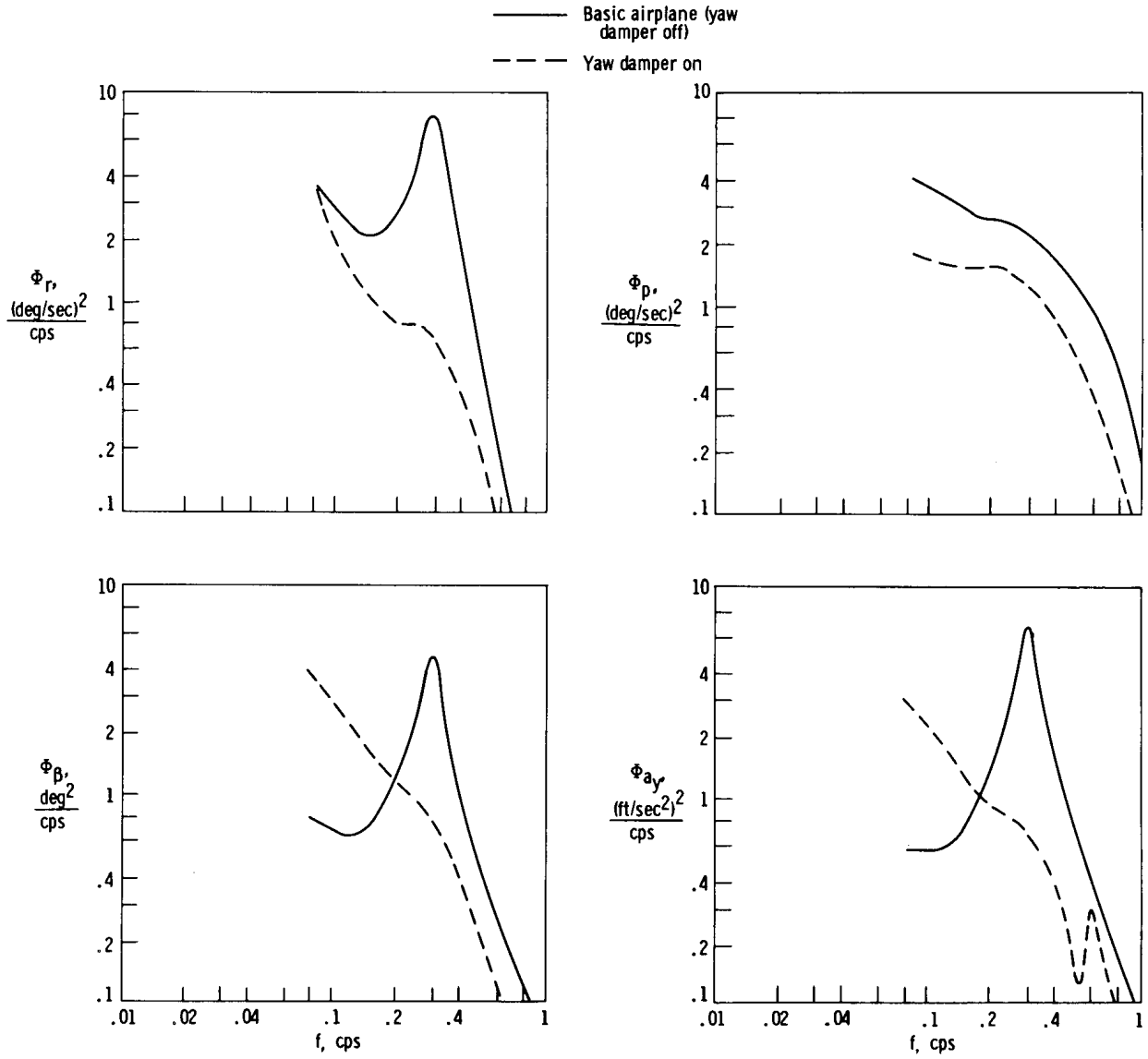

Figure 10. Flight-test results showing the comparison of airplane power spectra with and without the yaw damper for the approach configuration in moderate turbulence. V_i = 80 knots; $\delta_f = 27^o$; gear down; n = 60.

The effect of the yaw damper on the pilot's workload during an ILS approach in turbulent air was also evaluated. The pilots used hoods and partial windshield masks to simulate IFR conditions during the approach to an altitude of 200 feet. Conventional general-aviation glide-slope and localizer displays were used for steering information. In figures 11 and 12, several parameters recorded during an ILS approach in moderate

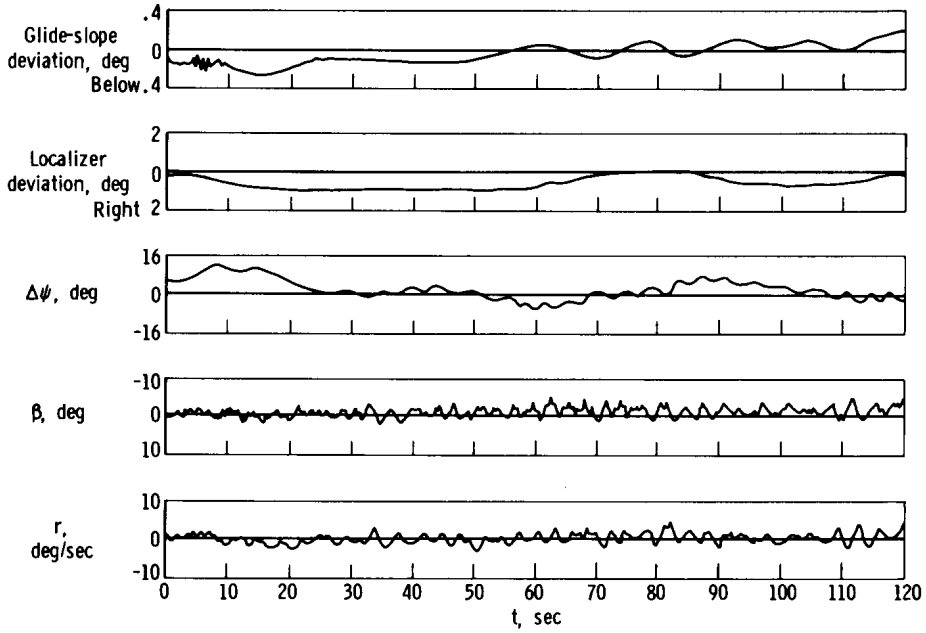

Figure 11. Basic airplane (yaw damper off) ILS approach in moderate turbulence. V_i = 100 knots; $\delta_f = 27^o$; gear down.

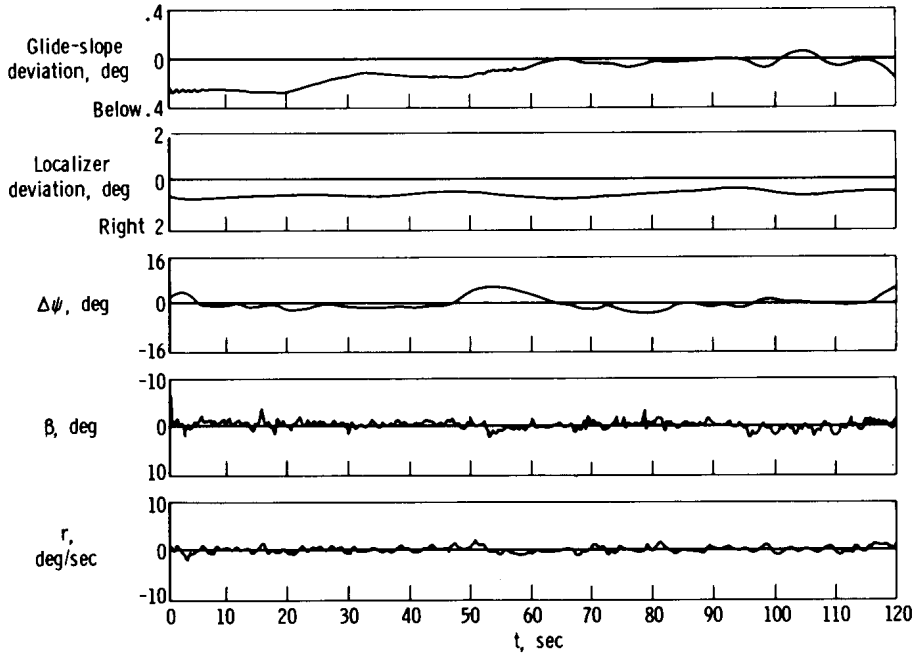

Figure 12. ILS approach in moderate turbulence with yaw damper. V_i = 100 knots; $\delta_f = 27^o$; gear down.

turbulence are shown as a function of time for damper-off and damper-on configurations, respectively. The Dutch roll oscillations excited by the gust disturbances are apparent in the yaw-rate and sideslip traces. The constant-heading oscillation of ±2° in figure 11 is a result of the Dutch roll motion. This oscillation was not present when the damper was operating, as shown in figure 12. The pilots generally thought that the ILS approaches were easier to make with the yaw damper on, although they believed that they were still difficult to accomplish and that there was little significant improvement in the overall pilot performance. This is also indicated by lack of significant differences in the glide slope and localizer deviations for the damper-on and damper-off ILS approaches shown in figures 11 and 12.

Aircraft power spectra for the two approaches are presented and compared in figure 13. The reduction in Dutch roll motion produced by the yaw damper is indicated

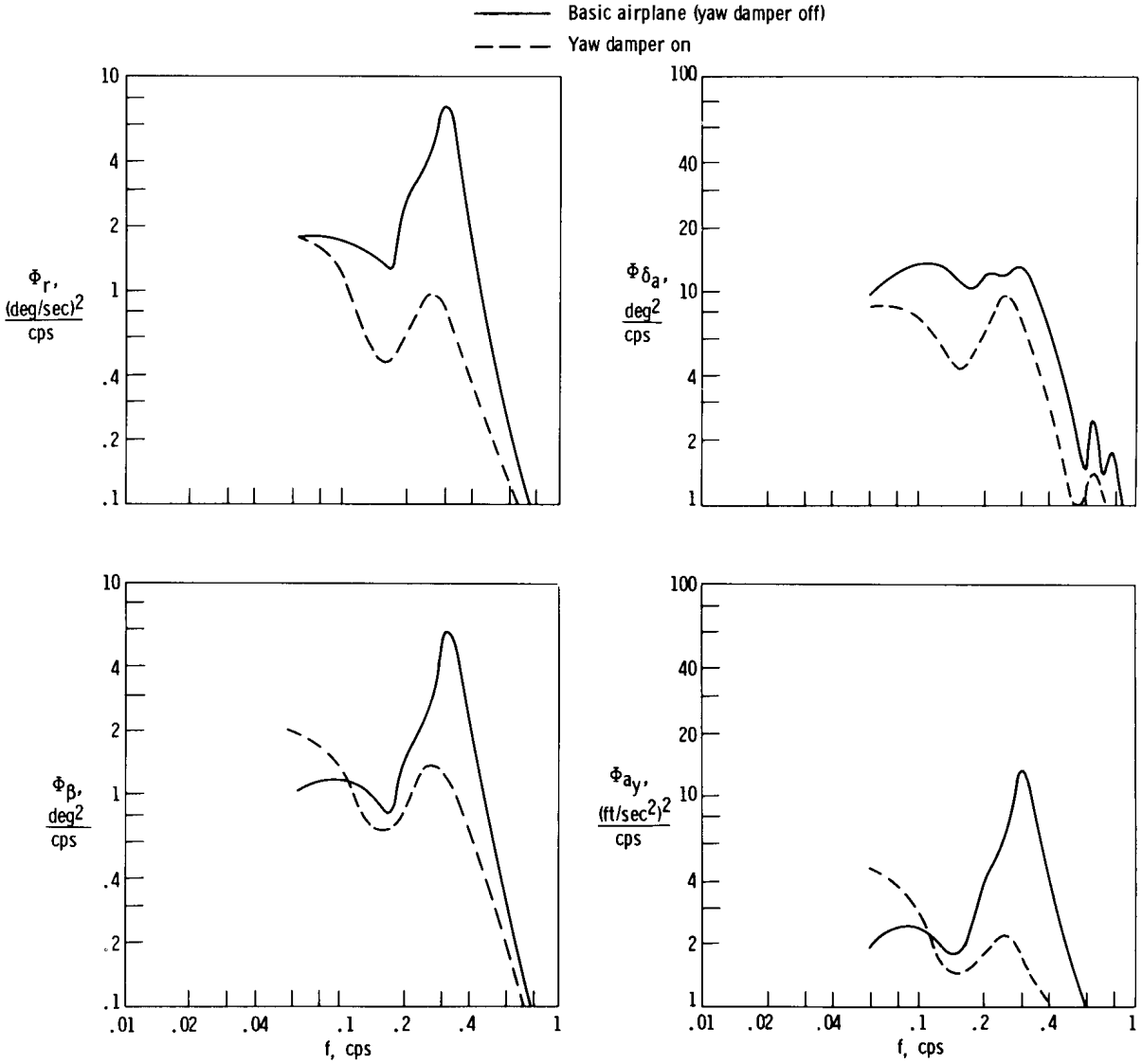

Figure 13. Flight-test results showing the comparison of airplane power spectra with and without the yaw damper for an ILS approach in moderate turbulence. V_i = 100 knots; $\delta_f = 27^o$; gear down; n = 60.

by the differences in the power spectra at the Dutch roll frequency. The increases in sideslip and lateral-acceleration motions produced by the yaw damper at the lower frequencies are again apparent. The $\bar{\Phi}_{\delta_a}$ curve for the approach with the yaw damper on shows measurably less power dissipation than for the basic airplane, indicating less aileron motion. Since the aileron motion for these two approaches was due entirely to pilot inputs, the indication is that the pilot was working somewhat less during the yaw-damper-on approach than during the basic-airplane approach. This tends to agree with the pilots' comments that the ILS approaches with the damper on were easier to accomplish, although the improvement was not significant. Use of the yaw damper during an ILS approach generally resulted in an improvement in pilot rating of less than one number (based on the scale in table 2).

Adverse-yaw characteristics. – The roll-yaw coupling characteristics of the test airplane and the effect of the yaw damper and the aileron-to-rudder interconnect are shown in figure 14. For these tests the airplane was in the cruise configuration and flying at a speed of 100 knots. No attempt was made by the pilot to coordinate the rudder with the aileron. Adverse aileron yaw for the basic airplane is illustrated in figure 14(a), which is a time history of the response to aileron deflections. For 17° aileron pulses, the resulting sideslip angle is on the order of 3° for this flight condition. Sideslip excursions on the order of 5° occur coincident with the aileron inputs for the damper-on, interconnect-off configuration (fig. 14(b)). The effect of the interconnect in alleviating the sideslip excursions is shown in figure 14(c).

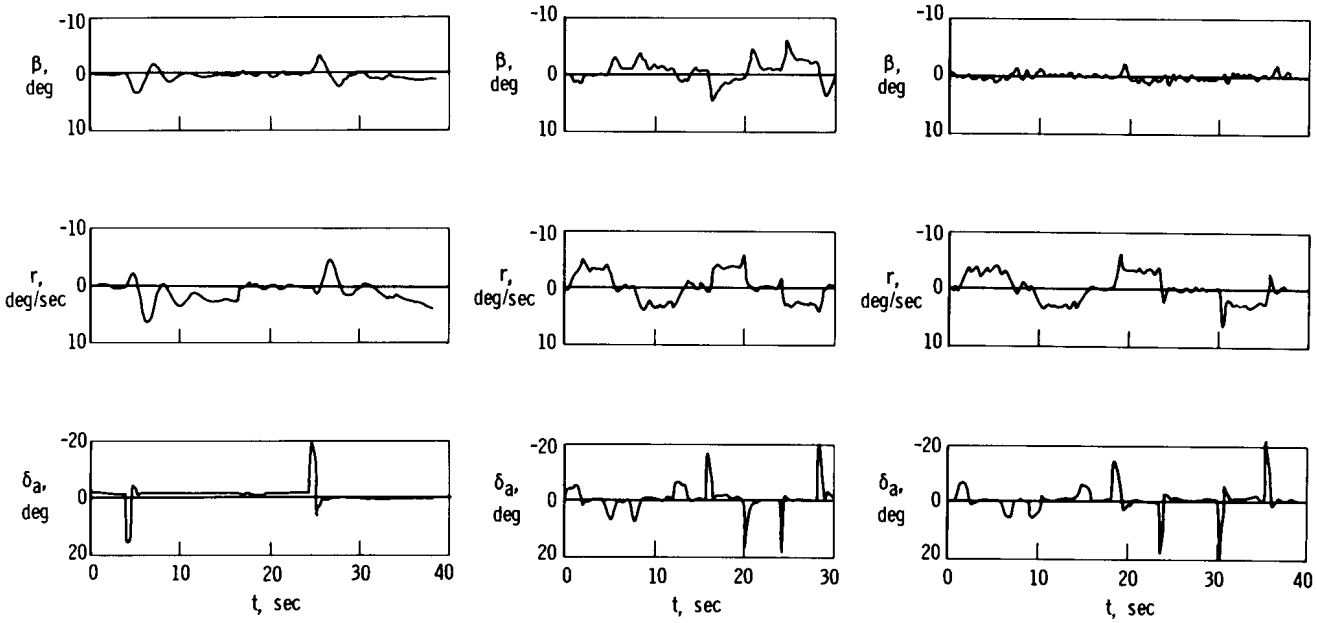

(a) Basic airplane (yaw damper off).

(b) Yaw damper only.

(c) Yaw damper and interconnect.

Figure 14. Response of test airplane to aileron pulses with and without yaw damper and aileron-to-rudder interconnect. Cruise configuration; V_i = 100 knots.

In general, the pilots found the aileron-to-rudder interconnect to be effective in providing directional quickening, particularly during instrument flight, thereby allowing small heading changes to be made faster and more accurately than without the interconnect. Accurate rollouts on heading were also markedly easier to accomplish, and the adverse-yaw characteristics of the test airplane were considerably improved with the interconnect.

Stall and recovery characteristics. – Stalls were performed at an altitude of 6000 feet with the airplane in the cruise configuration and the engine power set for level flight. The yaw-rate damper had a favorable effect on the stall motions of the airplane. This is illustrated in figure 15, which shows data from two stall maneuvers, one performed without the damper and one performed with the damper on. Stall onset is indicated by a vertical line. Aileron and elevator controls were used freely and instinctively; the rudder was not used.

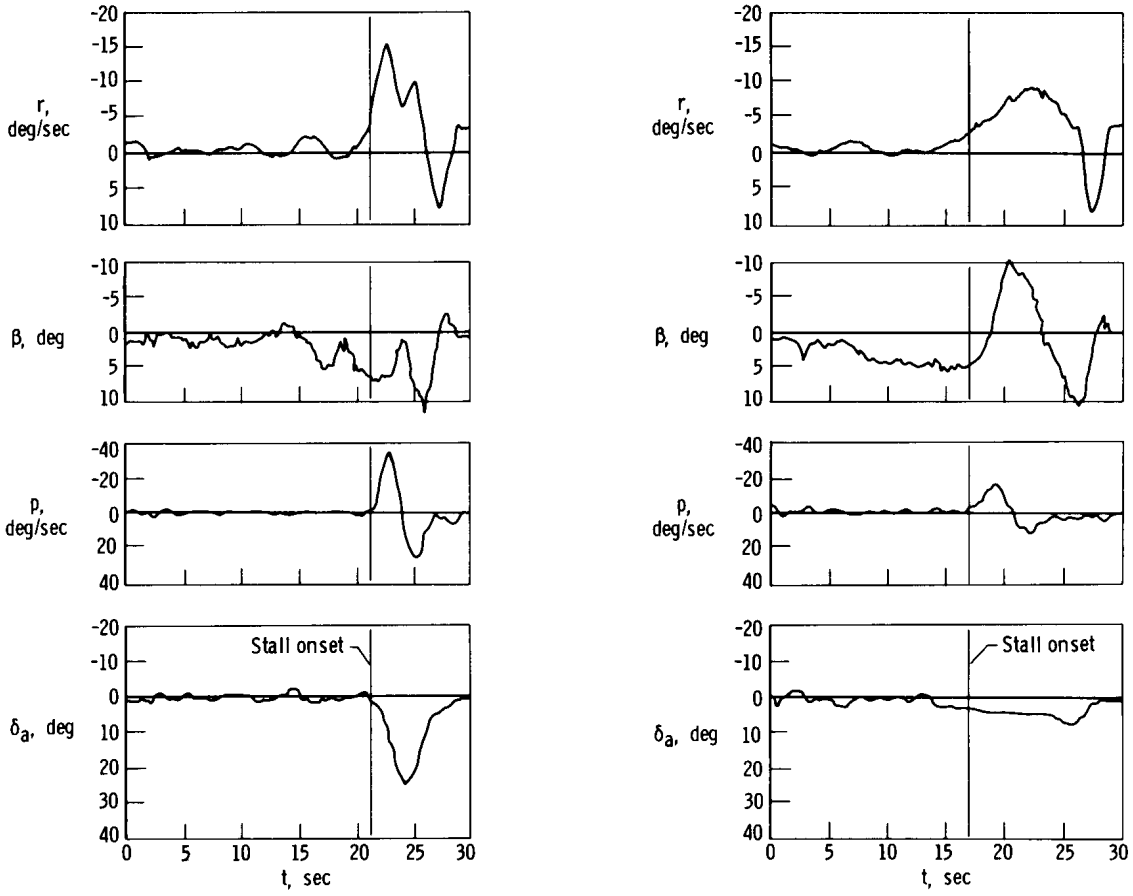

(a) Basic airplane (yaw damper off). *(b) Yaw damper on.*

Figure 15. Effect of yaw damper on test airplane stall motions. Cruise configuration; altitude, 6000 ft; cruise power.

For the basic airplane, at the instant of stall onset, a rapid rolling and yawing motion occurred, and the pilot rapidly applied 25° of aileron. Peak roll and yaw rates of -32 degrees per second and -15 degrees per second, respectively, were generated before the initial direction of the motion was reversed.

The same maneuver was performed with the yaw damper engaged. The maximum roll and yaw rates were reduced appreciably, and the pilot had more time to take corrective action. The peak yaw rate of 8 degrees per second occurred 6 seconds after stall onset, and the peak roll rate of 15 degrees per second occurred 3 seconds after onset. It should also be noted that the corrective action made by the pilot was minor compared to that made with the basic airplane. Only 7° of aileron was applied a full 8 seconds after stall onset. The factor reducing the airplane motion was the rudder deflection resulting from the yaw damper, which was in a direction to arrest the initial yawing motion. Although the damper effectiveness was not great enough to completely arrest the yaw rate, the yawing acceleration was greatly reduced, along with the yaw-induced roll.

Characteristics for simulated engine failure. – Power failure was simulated by rapidly reducing one throttle to the idle-power position. The pilot was instructed not to initiate recovery procedures until he felt it necessary. In figure 16 the effect of the yaw damper on airplane motions resulting from a simulated in-flight engine power failure is shown. With the damper off, both rudder and aileron recovery inputs were applied by the pilot 3 seconds after the throttle was chopped. A maximum yaw rate of 15 degrees per second was still achieved, however. With the damper on, the pilot did not initiate recovery until 6 seconds after power loss, and the maximum yaw rate was smaller. The recovery time available to the pilot, then, was effectively doubled by the increased yaw damping.

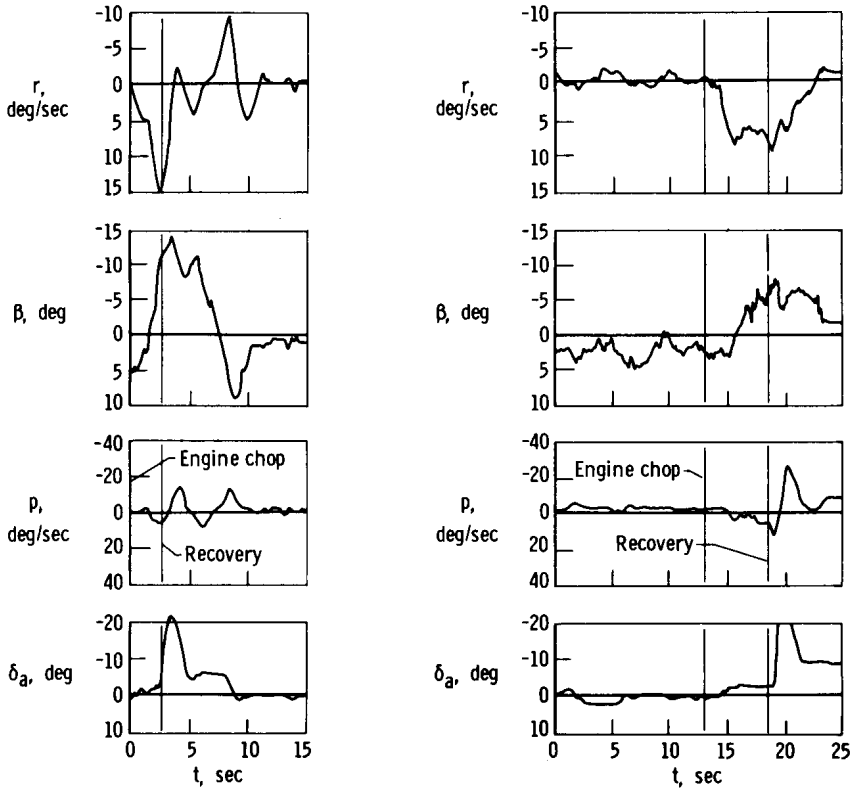

(a) Basic airplane (yaw damper off). *(b) Yaw damper on.*

Figure 16. Effect of yaw damper on airplane motions following a simulated engine failure.

Effect on Autopilot Performance

The effect of the yaw damper on the heading-hold autopilot closed-loop performance is shown for two flight conditions in figures 17 and 18. Figures 17(a) and (b) show the test airplane responses to rudder releases from steady-state sideslips with the airplane in the cruise configuration at a speed of 140 knots. In this instance, the autopilot was effective in maintaining aircraft heading and showed satisfactory transient response

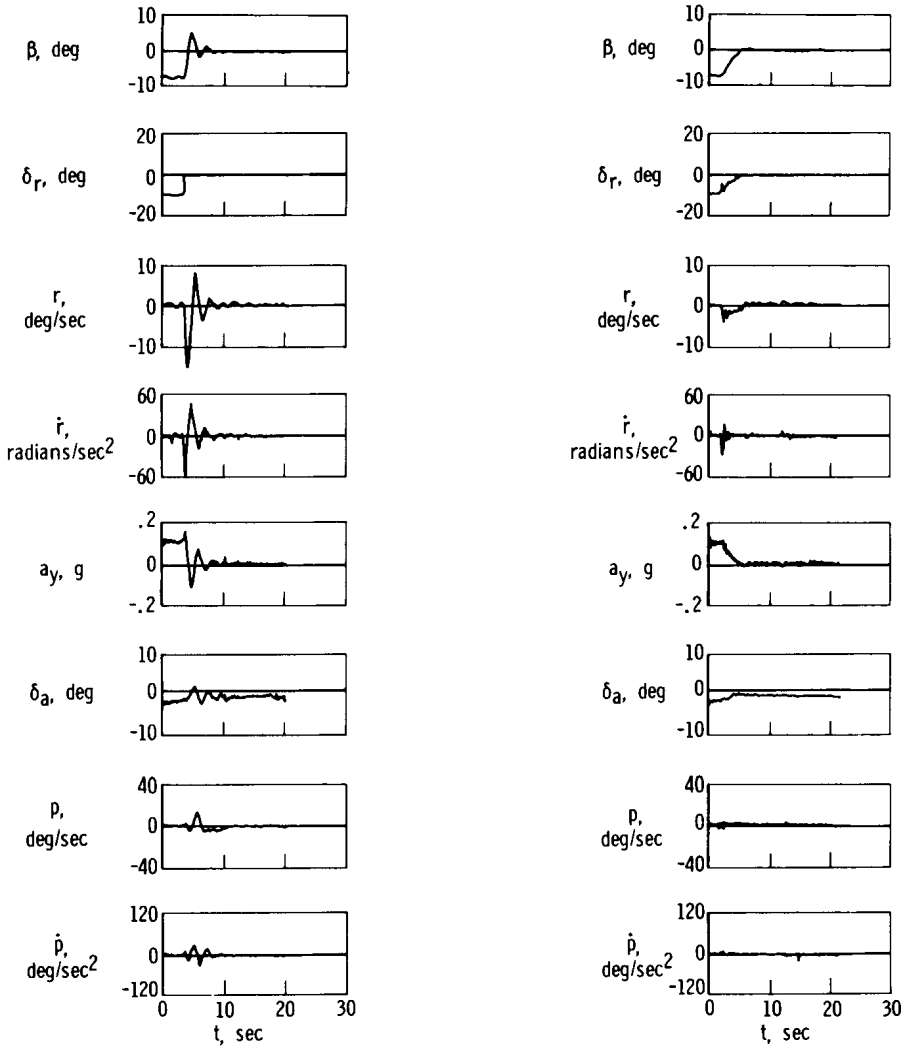

(a) Heading-hold autopilot on, yaw damper off.

(b) Heading-hold autopilot and yaw damper on.

Figure 17. Test airplane response to a rudder release from a steady sideslip with the heading-hold autopilot engaged, with and without yaw damper. Cruise configuration; V_i = 140 knots.

characteristics. Figures 18(a) and (b) illustrate the deterioration in autopilot performance at the lower velocities with the airplane in the approach configuration. For this particular maneuver, a steady-state sideslip release at 80 knots, the Dutch roll

damping had decreased to 0.03. The stabilizing influence provided by the yaw damper is illustrated in figure 18(b).

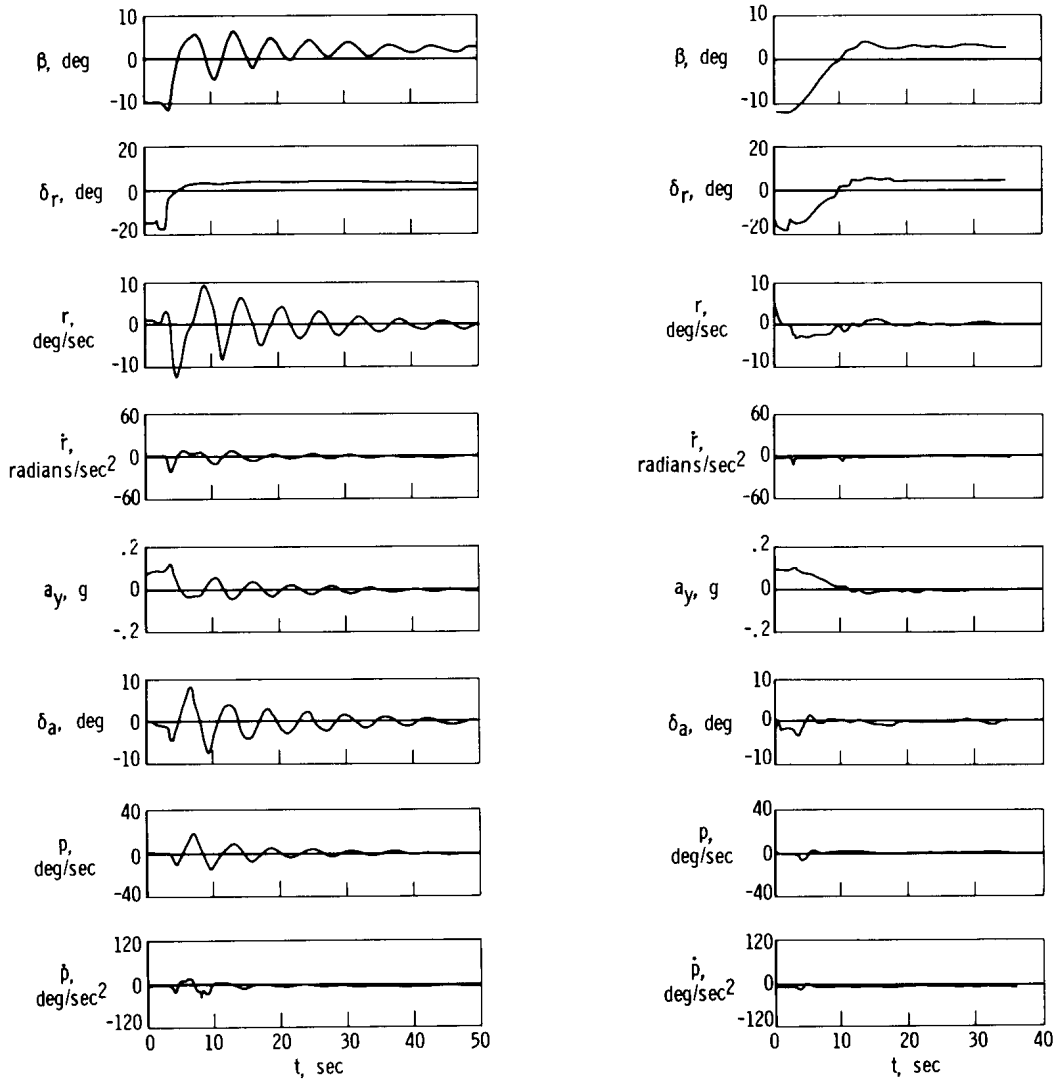

(a) Heading-hold autopilot on, yaw damper off.

(b) Heading-hold autopilot and yaw damper on.

Figure 18. Test airplane response to a rudder release from a steady sideslip with the heading-hold autopilot engaged, with and without yaw damper. Approach configuration; V_i = 80 knots; $\delta_f = 27^o$; gear down.

In figure 19 a comparison is shown of aircraft power spectra with and without the autopilot heading-hold mode operating for the approach configuration in moderate turbulence and at a speed of 80 knots. The power spectra show that, with the heading-hold mode on, the airplane's Dutch roll motions were much greater in turbulence than the motions experienced without the heading-hold mode in turbulence of the same intensity level. However, it should be noted that, even though the Dutch roll motions in turbulence were more prevalent with the autopilot system engaged, the positive

roll (spiral) stability provided was greatly appreciated by the pilots. A similar situation was found for the wings-leveler autopilot mode.

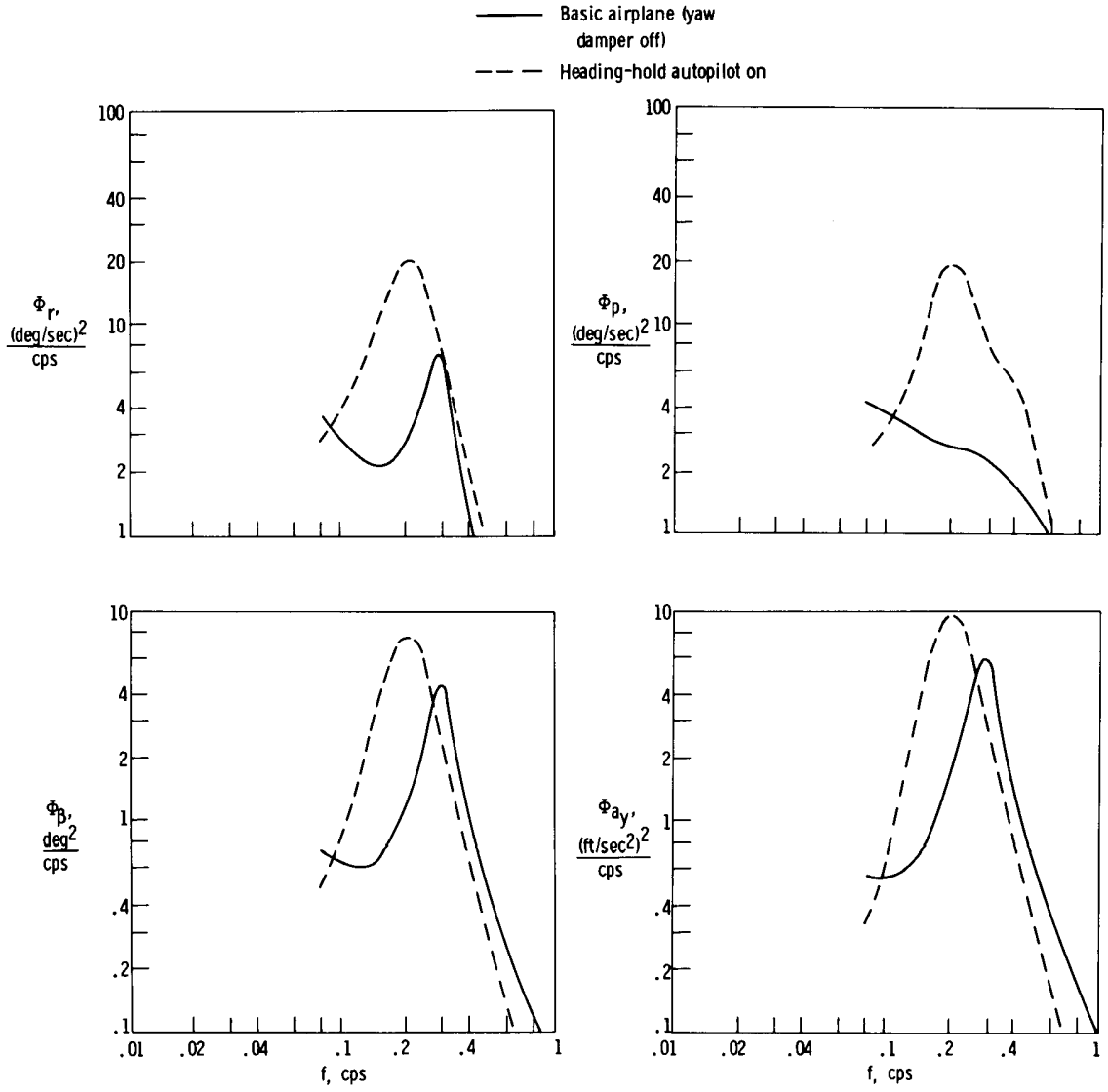

Figure 19. Flight-test results showing the comparison of airplane power spectra with and without the heading-hold autopilot for the approach configuration in moderate turbulence. V_i = 80 knots; $\delta_f = 27^o$; gear down; n = 60.

The effect of the yaw damper in reducing the oscillatory motions experienced with the autopilot in turbulence is shown by the power-spectral-density comparison in figure 20. The oscillatory peaks occurring with the autopilot on at 0.2 cps are considerably attenuated by use of the yaw damper. There is, however, the resultant

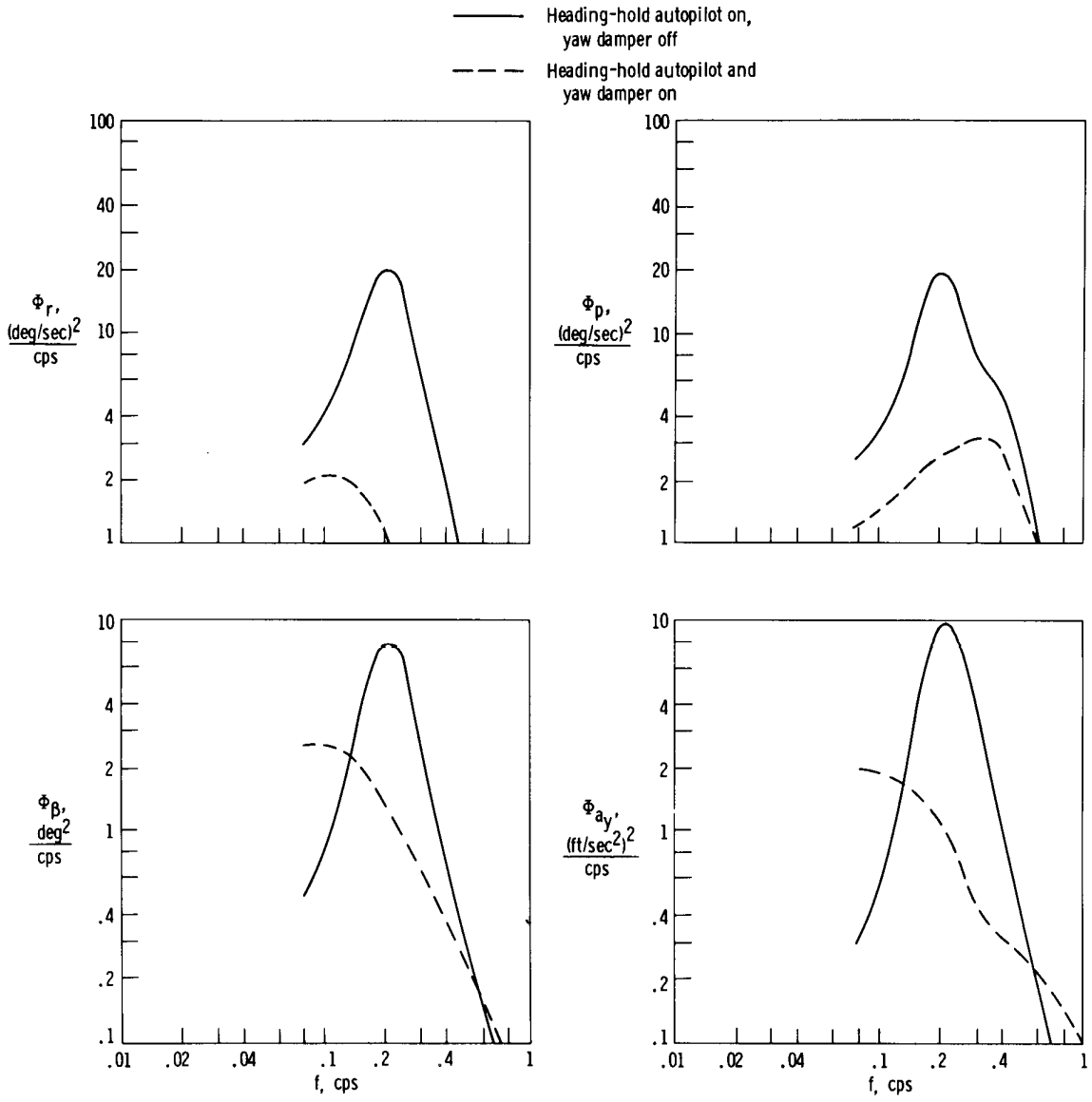

Figure 20. Flight-test results showing the comparison of airplane power spectra with the heading-hold autopilot, with and without the yaw damper, for the approach configuration in moderate turbulence. V_i *= 80 knots;* $\delta_f = 27^o$*; gear down;* $n = 60$.

increase in low-frequency angle of sideslip and lateral-acceleration motion, as was discussed previously. In figure 21, aircraft power spectra for an ILS approach made with the heading-hold autopilot coupled to the localizer are compared to the power spectra for a similar ILS approach in which the yaw damper and aileron-to-rudder interconnect were included. The significant reduction in aircraft motion experienced with the yaw damper is apparent, except for the low-frequency increases in sideslip and lateral acceleration. The improvement in both yaw rate and roll control input is appreciable.

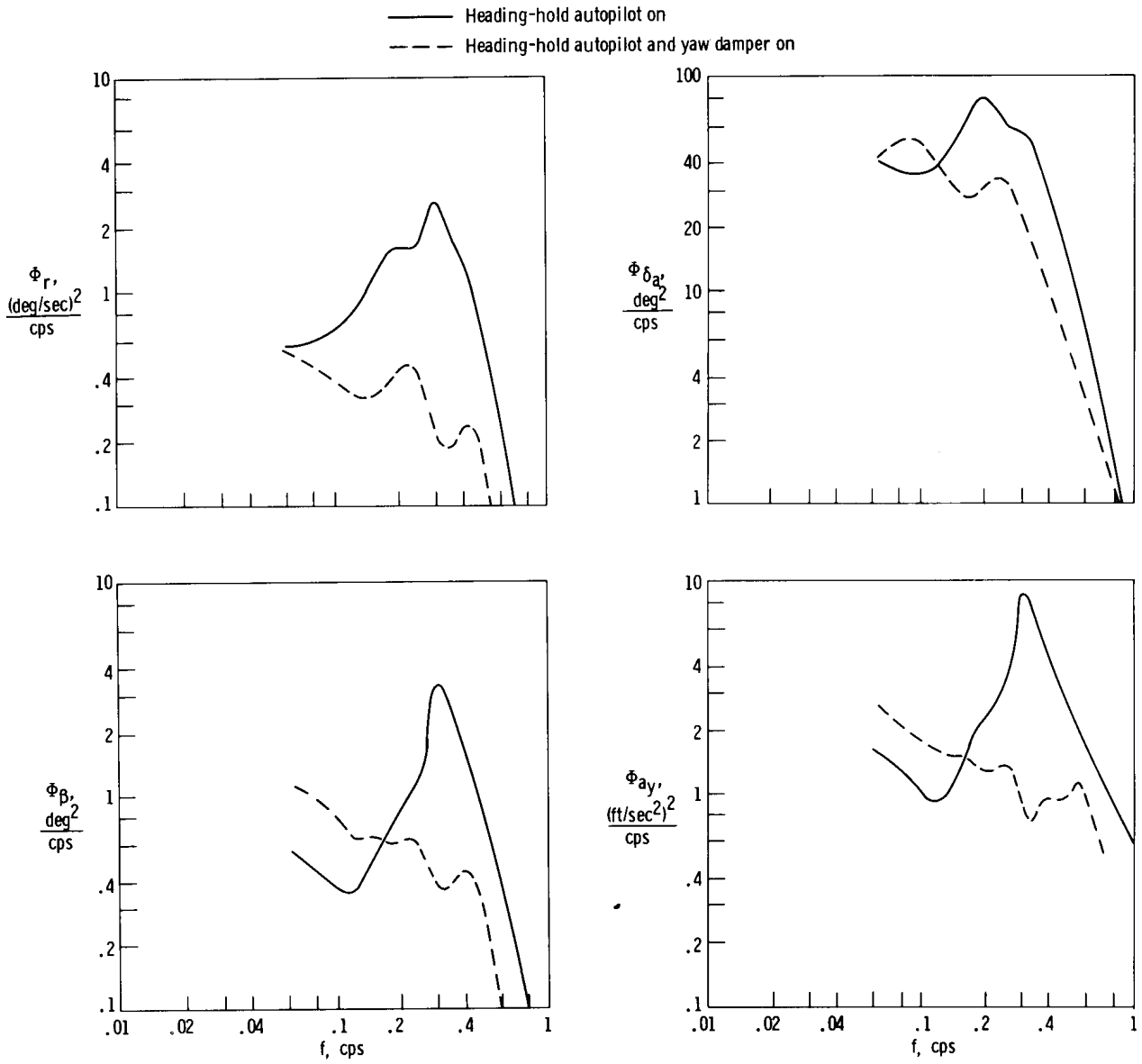

Figure 21. Flight-test results showing the comparison of airplane power spectra with the heading-hold autopilot and the heading-hold autopilot with the yaw damper for an ILS approach in moderate turbulence. V_i = 100 knots; $\delta_f = 27^o$; gear down; n = 60.

It is interesting to note that in reference 4 the use of autopilot systems in turbulence is strongly recommended, primarily because of the reduction in inadvertent structural overloading which sometimes occurs during flights in turbulent air. This effect was attributed to the increased damping of the short-period motion of an airplane when an autopilot is used. However, the autopilot in the test airplane produced no significant improvement in the short-period characteristics of the airplane. Instead, at the lower approach velocities, the airplane's Dutch roll frequency approached the natural frequency of the autopilot, resulting in oscillations of higher amplitude than would be experienced with the autopilot disengaged. This is shown in figure 22 by the summaries of the overall root-mean-square intensities of lateral-directional parameters for the various operating modes during level flight in light-to-moderate turbulence

with the airplane in the cruise and the approach configurations. The root-mean-square intensity value for each parameter was obtained by taking the square root of the area beneath the corresponding power-spectral-density plots. A frequency range of 0.0625 cps to 1.0 cps was used. It is evident that the autopilot in the test airplane did not meet the basic requirements assumed in reference 4. The highest intensity level for each parameter was that obtained with the autopilot operating. It should be emphasized that, for these level-flight evaluations in turbulence, the pilot was instructed to apply only minimal control inputs so that actual airplane and system performance could be approximated.

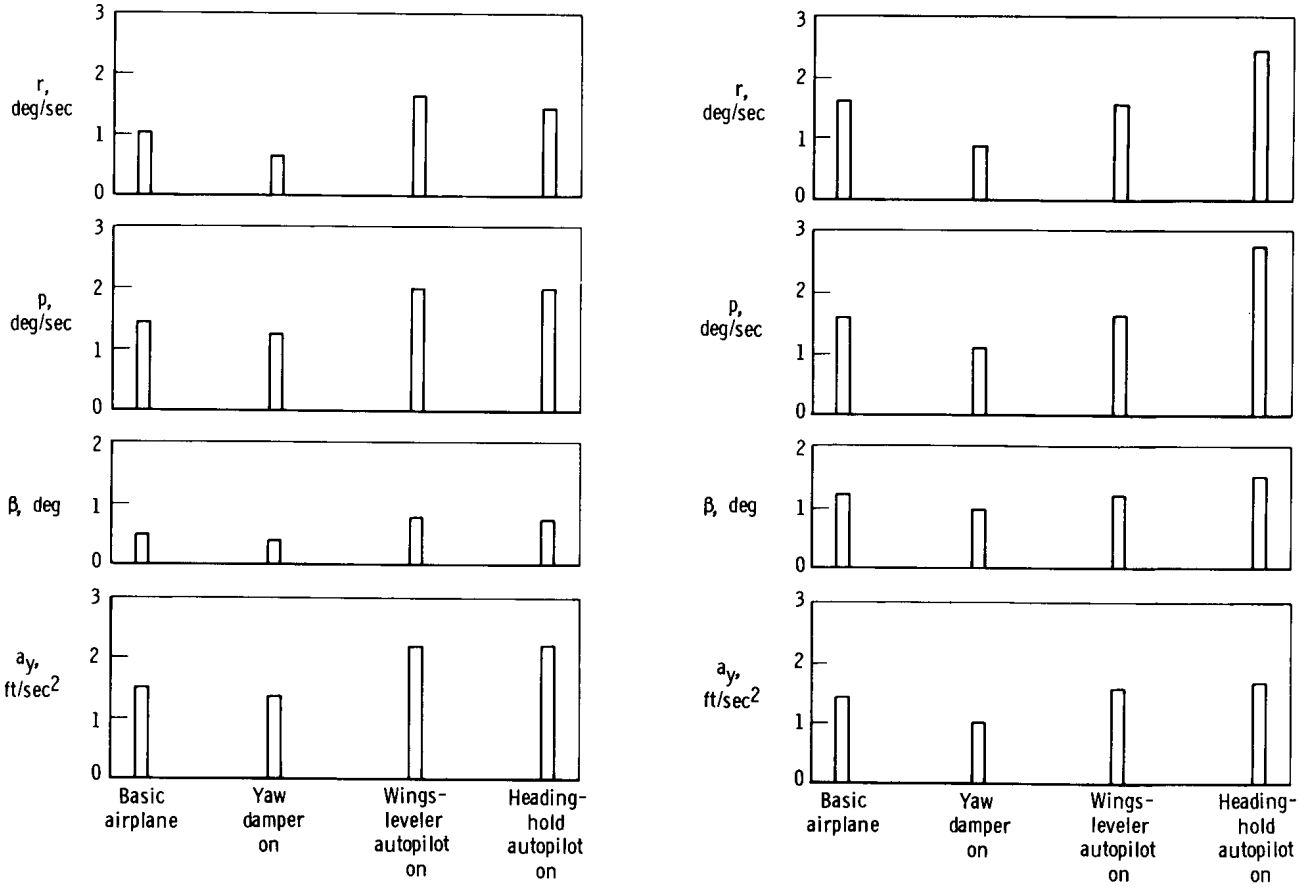

(a) Cruise configuration. *(b) Approach configuration.*

Figure 22. Total root-mean-square intensities of airplane motions for level flight in light-to-moderate turbulence in the cruise and approach configurations.

Comparison With Lateral-Directional Criteria

The Dutch roll characteristics of the test airplane are compared in figure 23 with the lateral-directional criterion given in reference 5. Although this criterion was not developed specifically for this type of airplane, it does serve as a basis for comparing the effect of the yaw damper and autopilot on the lateral-directional characteristics of the test airplane. The Dutch roll characteristics of the airplane were marginally acceptable, on the basis of the referenced criterion. The autopilot resulted in a deterioration of Dutch roll characteristics to the extent of being unacceptable. The

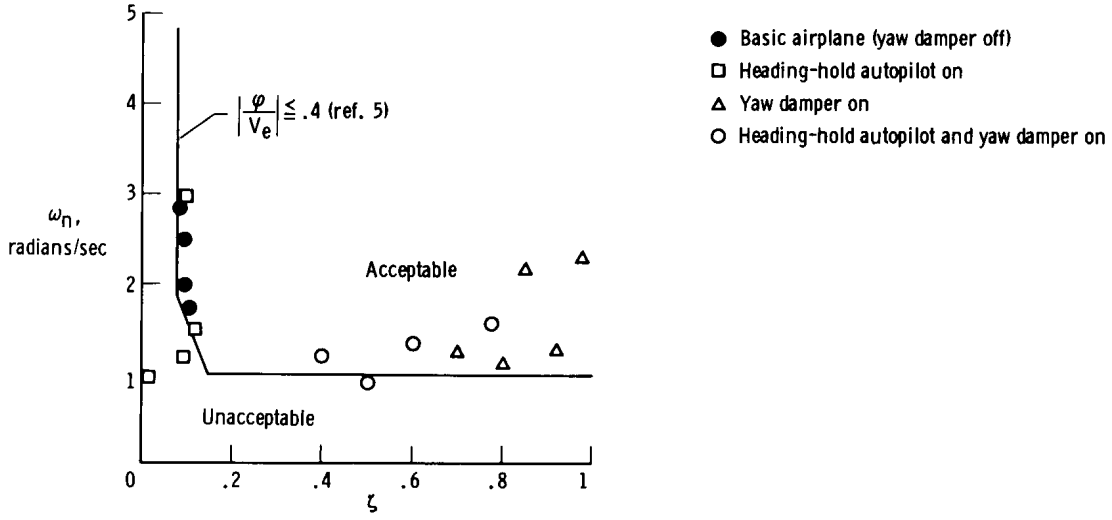

Figure 23. Effect of yaw damper and autopilot on the test airplane lateral-directional oscillations.

improvement effected by the yaw damper for both the basic airplane and the basic airplane with the autopilot is apparent in the figure.

Pilot Opinion Summary

Pilot ratings were obtained to evaluate the relative difference in both ride and flying qualities of the test airplane for the several configurations. Fifteen pilots participated in the evaluation. Their backgrounds and flight experiences are summarized in table 3. Pilot comments on the overall flying qualities of the test airplane were also obtained and are summarized in appendix D. Pilot ratings of flying qualities were based on the rating scale presented in table 2. Ride-quality ratings, obtained from both pilots and passengers, were based on the rating scale shown in table 4.

Handling-qualities ratings. – Pilot ratings are presented in figure 24 for maneuvering flight and constant-heading tasks. The data points indicate the average rating for a particular task, and the arrows indicate the spread in the ratings for all pilots. Banked turns were made with slow and fast turn entry roll rates. When this task was performed with the basic airplane, both aileron and rudder controls were used by the pilot for turn coordination. Only ailerons were used when the yaw damper was engaged. The normal bank-angle and heading-change control knobs on the autopilot console were used when the autopilot system was engaged.

As shown in figure 24, for maneuvering flight in the cruise configuration, the average rating for the basic airplane was 3.5; for the yaw damper operating, the average rating was approximately 2.5, about a one-rating improvement. The same general effect of the yaw damper is shown for the wings-leveler autopilot. Slightly less improvement was noted with the yaw damper on when the heading-hold system was used. The same general trend was experienced for the constant-heading task, with slightly better overall ratings obtained.

The averaged pilot ratings and corresponding spread for three instrument-flight tasks performed with the test airplane in the approach configuration are shown in

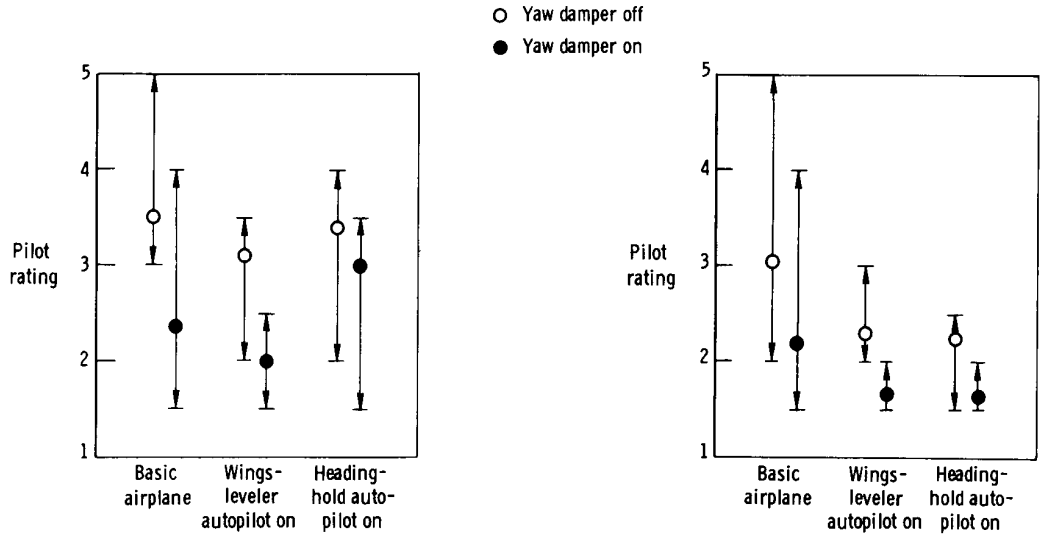

(a) Maneuvering flight. *(b) Constant heading.*

Figure 24. Summary of pilot ratings for maneuvering flight and constant-heading tasks. Cruise configuration; light-to-moderate turbulence.

figure 25. For the ILS approach task (fig. 25(a)), a pilot rating improvement of less than one number was experienced with the use of the yaw damper. As noted previously,

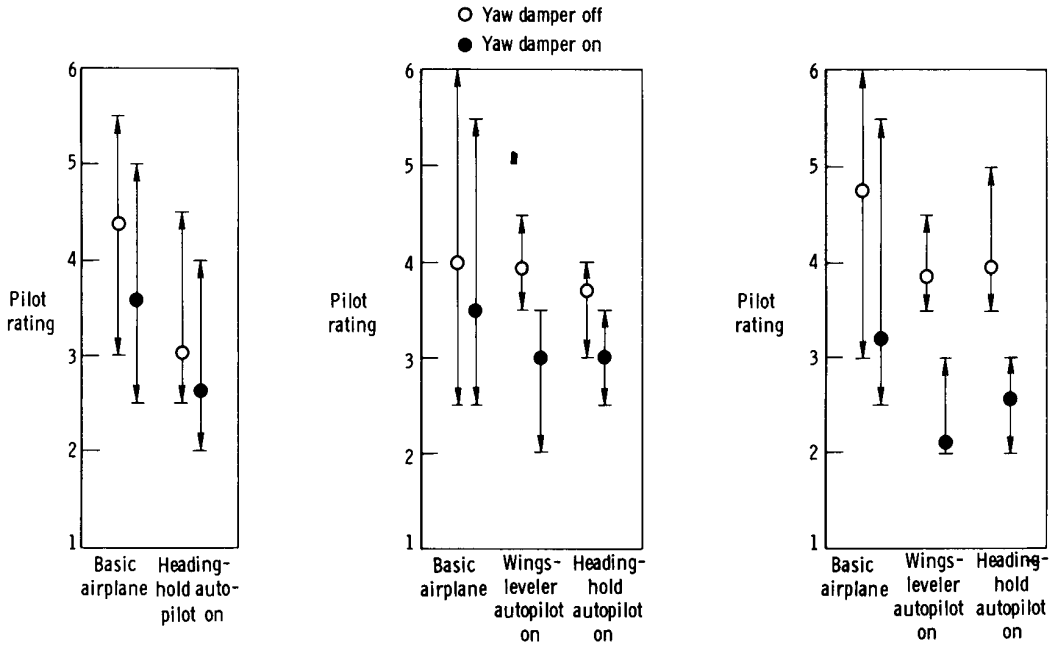

(a) ILS approach. *(b) Maneuvering flight.* *(c) Constant heading.*

Figure 25. Summary of pilot ratings for three instrument-flight tasks. Approach configuration; light-to-moderate turbulence.

even though the lateral-directional oscillations were greater for approaches made with the heading-hold autopilot on, this mode was rated significantly better by the evaluation pilots. This indicates that the pilots were not so much concerned with the oscillatory motions as with the average heading angle for this task. They were willing to forego corrections for short-period disturbances as long as they were assured that the average heading would always be maintained.

The degree to which an improvement was noted was found to depend to a large extent on how tightly a pilot normally controlled yawing motions during an approach. One pilot, for example, believed that the short-period yawing motion could be completely ignored during an ILS approach in turbulence; therefore, he did not see any improvement with the increased damping. Other pilots, tending to control heading and yawing motion more tightly, found the yaw damper to be beneficial in reducing the motions and improving the pilot's control task. The degree of improvement was also found to vary markedly from one pilot to another, depending on background and experience. Military pilots, for instance, with primarily jet-aircraft experience found the lack of required rudder-pedal inputs with the damper and aileron-rudder interconnect to be agreeable, whereas pilots with primarily general-aviation experience found flying with their feet on the floor unnatural and difficult to adjust to even though no inputs were required. Most pilots agreed that the rudder-pedal motion resulting from the parallel summing arrangement between pilot and damper inputs was undesirable and distracting, especially in turbulence. Isolation of rudder pedals from damper inputs was considered to be a highly desirable feature.

For the maneuvering-flight task in the approach configuration (fig. 25(b)) the pilot-rating trends were the same as those experienced in the cruise configuration (fig. 24(a)). The yaw damper was rated about one-half to one pilot rating better when used with the basic airplane, wings leveler, or heading-hold systems. For the constant-heading task (fig. 25(c)), the damper shows a 1.5 to 2 pilot-rating improvement when used with the basic airplane, wings-leveler, or heading-hold systems.

Ride-quality ratings. – A summary of ride-quality ratings is presented in figure 26. The ratings were obtained for a light-to-moderate level of turbulence for the approach

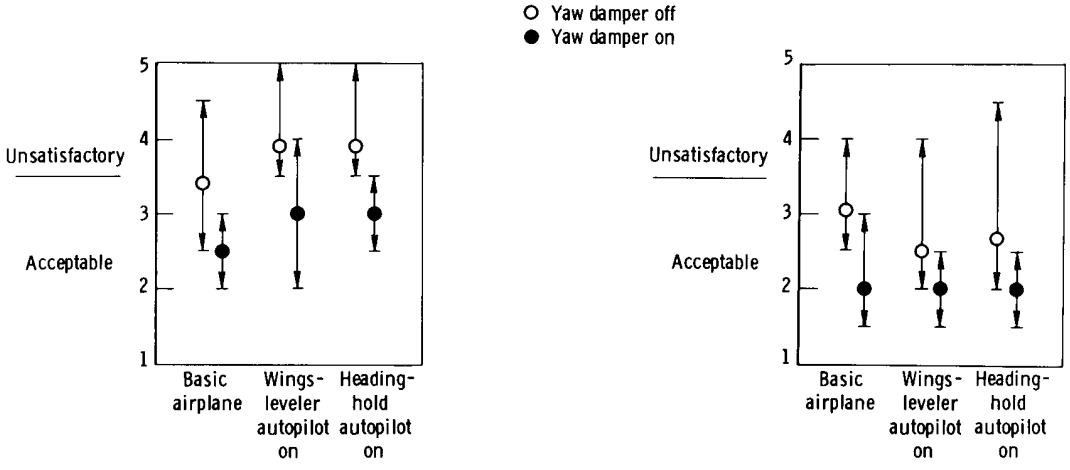

(a) Approach configuration. *(b) Cruise configuration.*

Figure 26. Summary of ride-quality ratings for the approach and cruise configurations in light-to-moderate turbulence.

and cruise configurations and for several system modes. All ratings were obtained within the same hour and over specified geographical boundaries to insure minimum variations in turbulence intensities and spectral content. As shown in the figure, there was some improvement in the overall ride qualities of the test airplane when the yaw damper was used. The most noticeable improvement was in the approach configuration in which the airplane was rated marginally acceptable to unsatisfactory without the damper for all control modes, and acceptable with the damper engaged.

CONCLUDING REMARKS

A yaw damper and aileron-to-rudder interconnect system was installed in a light twin-engine, general-aviation type of airplane to evaluate the effect of increased Dutch roll damping on the flying qualities, primarily in turbulence. A flight-test program was conducted in which 15 evaluation pilots participated. Results of a previous study (NASA TN D-3726) indicated that poor Dutch roll damping, which is characteristic of this class of aircraft, might contribute significantly to the heavy pilot work load during ILS approaches in turbulence. Results of the present study, however, showed that Dutch roll damping did not affect handling qualities of the test airplane as significantly as was suggested in the previous study. Even when the lateral-directional oscillations were essentially eliminated, the ILS approach task in turbulence was difficult for experienced pilots.

Results from the flight-test program showed that the yaw damper and aileron-to-rudder interconnect system on the test airplane improved the overall lateral-directional handling qualities of the airplane in turbulence. The Dutch roll motions for both the approach and cruise configurations in turbulence were significantly reduced, and turns could be made faster, more accurately, and easier as a result of the aileron-to-rudder interconnect.

Pilot workload during ILS approaches in moderate turbulence was less with the yaw damper engaged than when it was not in operation. The actual performance, however, in accomplishing the approach maneuver was not significantly improved. The degree to which the decrease in workload was appreciated was found to depend largely on individual piloting technique and background.

The yaw damper was effective in reducing the maximum roll and yaw rates normally encountered during stalls with the test airplane. The damper provided the pilot with more time to take corrective action after stall onset, and the degree of corrective action was small compared to stalls performed without the damper.

Airplane motions resulting from a simulated in-flight engine-power failure were considerably reduced with the yaw damper on and, as in the stall maneuvers, the pilot had approximately twice as much time in which to take corrective action.

An increase in the intensity of the lateral motions of the test airplane in turbulence was experienced when the autopilot system was used alone. A significant improvement was achieved in autopilot performance during cruising flight and ILS approaches in moderate turbulence by the addition of the yaw-rate damper loop.

The riding qualities of the test airplane in turbulence were improved when the yaw damper was engaged. The improvement was most noticeable in the approach configuration, in which the airplane was rated marginally acceptable to unsatisfactory for all control modes without the damper and acceptable with the damper.

Flight Research Center,
National Aeronautics and Space Administration,
Edwards, Calif., March 20, 1970.

APPENDIX A

YAW-DAMPER DESIGN

HINGE-MOMENT CONCEPT

Figure 27 is a simplified block diagram of the hinge-moment yaw-damper system. The amount of steady-state yaw rate per rudder deflection for the basic airplane is primarily due to the N_{δ_r} derivative contained in the $\frac{r}{\delta_r}$ transfer function. Also, the

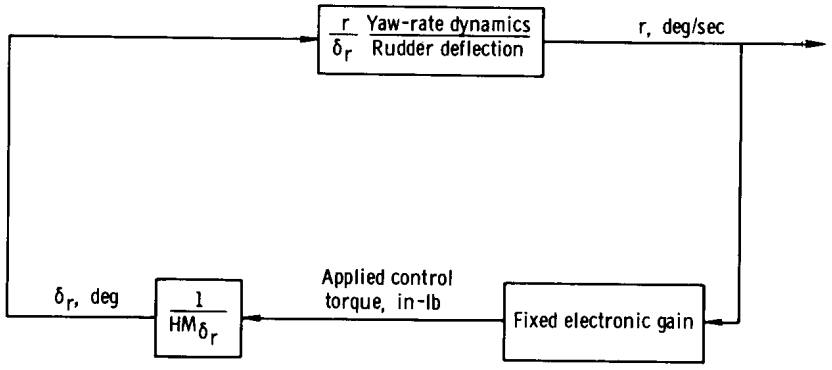

Figure 27. Simplified block diagram of hinge-moment yaw-damper system.

rudder deflection per applied torque at the actuator is inversely proportional to HM_{δ_r}. The relationship of rudder-control effectiveness and rudder hinge moment is examined in the following expressions:

$$N_{\delta_r} = C_{n_{\delta_r}} \frac{qSb}{I_Z}$$

$$HM_{\delta_r} = C_{h_{\delta_r}} qS_r\bar{c}_r$$

The ratio of control effectiveness to hinge moment results in the following relationship, which is independent of dynamic pressure:

$$\frac{N_{\delta_r}}{HM_{\delta_r}} = K_{constant} \frac{C_{n_{\delta_r}}}{C_{h_{\delta_r}}}$$

where

$$K_{constant} = \frac{Sb}{I_Z S_r \bar{c}_r}$$

APPENDIX A

Wind-tunnel and flight-test data for the test airplane show that $C_{n_{\delta_r}}$ and $C_{h_{\delta_r}}$ remain relatively constant with flight conditions and airplane configuration. Therefore, the open-loop gain of the system $\left(\frac{N_{\delta_r}}{HM_{\delta_r}} \text{ times the fixed electronic gain}\right)$ remains relatively constant with flight condition. Since there is not a large variation of yaw rate to rudder dynamic characteristics with flight condition, the closed-loop damping characteristics of the system are relatively invariant with flight condition.

Root-Locus Analysis

A cursory root-locus analysis was performed to determine the gain required in the yaw-damper electronics circuitry to provide adequate damping for the test airplane. Two flight conditions were investigated: landing approach and cruise. Values of the test airplane stability derivatives were obtained from wind-tunnel data for the airplane (ref. 6) where possible and estimated from flight data for three similar general-aviation aircraft when wind-tunnel data were inadequate. (See table 5.) The aircraft transfer function $\frac{r}{\delta_r}(s)$ was derived from linear, three-degree-of-freedom, perturbated equations referenced to the body axis. (See appendix B.)

A block diagram of the yaw-damper configuration used for the root-locus analysis is shown in figure 28. The transfer function of yaw rate to rudder $\frac{r}{\delta_r}(s)$ for the

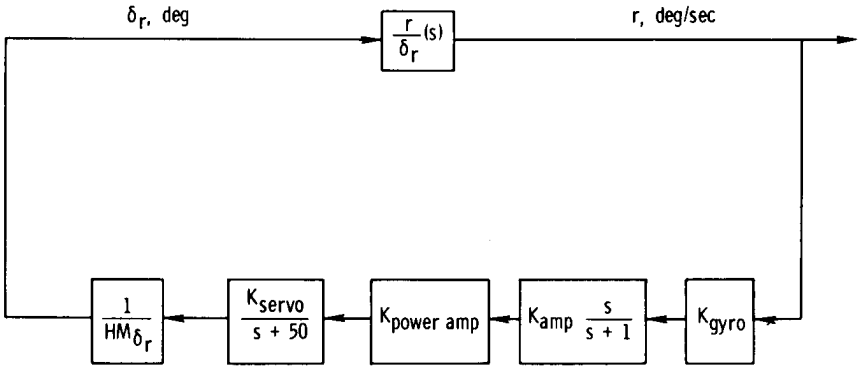

Figure 28. Block diagram of yaw-damper configuration for root-locus analysis.

landing configuration is given in the following expression:

$$\frac{r}{\delta_r}(s) = \frac{-1.96(s + 3.75)(s^2 + 0.058s + 0.26)}{(s - 0.04)(s + 3.66)(s^2 + 0.84s + 4.4)}$$

where the static gain of $\frac{r}{\delta_r}(s)$ is

$$N_{\delta_r} = -1.96 \text{ sec}^{-2}$$

APPENDIX A

The open-loop transfer function is given by the following expression:

$$G(s)H(s) = \frac{N_{\delta_r}}{HM_{\delta_r}} K_D \frac{s(s + 3.75)(s^2 + 0.058s + 0.26)}{(s - 0.04)(s + 1)(s + 3.66)(s + 50)(s^2 + 0.84s + 4.4)}$$

where the factor K_D is the damper electronic gain and is defined by the equation

$$K_D = K_{gyro} K_{amp} K_{power\ amp} K_{servo}$$

The quantity $\frac{N_{\delta_r}}{HM_{\delta_r}} K_D$ is the open-loop gain and is denoted by the symbol K_{OL}.

In figure 29 a root-locus plot of the yaw-damper response as a function of open-loop gain for the landing-approach configuration is presented. The Dutch roll damping increases to a maximum of about 0.7 at $K_{OL} = 200$ radians^{-1}. The Dutch roll natural frequency decreases to about 1.3 radians/sec. The damper gain K_D can be computed from the determined K_{OL} of 200 radians^{-1}.

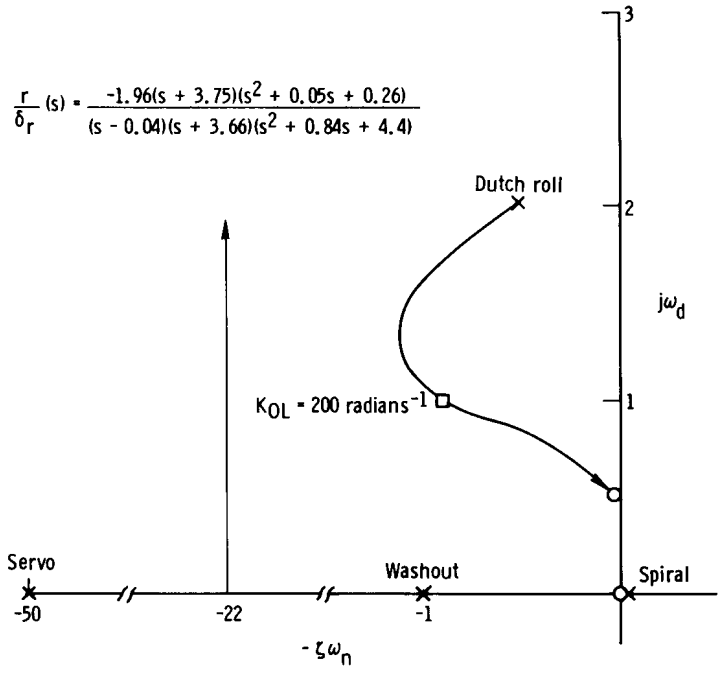

Figure 29. Root-locus diagram of yaw damper for approach condition.

The quantity $\frac{N_{\delta_r}}{HM_{\delta_r}}$, as mentioned earlier, is relatively independent of flight condition and is computed from information in table 5. Using the derivatives for the

approach condition results in the expression

$$\frac{N_{\delta_r}}{HM_{\delta_r}} = 0.002 \frac{\text{sec}^{-2}}{\text{in-lb}}$$

Therefore, since

$$K_{OL} = \frac{N_{\delta_r}}{HM_{\delta_r}} K_D$$

$$K_D = K_{OL} \left(\frac{HM_{\delta_r}}{N_{\delta_r}} \right)$$

Inserting known values for the right side of the preceding expression results in the following relationship:

$$K_D = (200 \text{ radians}^{-1})(500 \text{ in-lb sec}^2)$$

$$K_D = 100,000 \frac{\text{in-lb sec}}{\text{radians/sec}}$$

or, expressed in degrees,

$$K_D = 1750 \frac{\text{in-lb sec}}{\text{deg/sec}}$$

As shown in figure 28, the feedback transfer function is expressed in the form

$$\frac{K_D s}{(s + 50)(s + 1)}$$

By dividing the numerator and the denominator by 50, the transfer function can be expressed in the familiar frequency response form of

$$\frac{\frac{K_D}{50} s}{\left(\frac{s}{50} + 1\right)(s + 1)}$$

With the transfer function expressed in this (Bode) form, the steady-state damper gain $\frac{K_D}{50}$ is directly determined, as shown in the expression

$$\frac{K_D}{50} = 35 \frac{\text{in-lb sec}}{\text{deg/sec}}$$

APPENDIX A

In figure 30 the yaw-damper root-locus diagram for the cruise configuration is shown. For an open-loop gain of 200 radians^{-1}, the Dutch roll damping has increased to approximately 0.7 at a natural frequency of 3.5 radians/sec. Since $\frac{N_{\delta_r}}{HM_{\delta_r}}$ is relatively invariant with flight condition, the steady-state damper gain necessary to produce the 0.7 damping ratio is $35 \frac{\text{in-lb sec}}{\text{deg/sec}}$, which is equivalent to the damper gain determined for the landing-approach configuration. The natural frequency is higher, however, for cruising flight than for the landing-approach condition.

$$\frac{r}{\delta_r}(s) = \frac{-7.95(s + 6.72)(s^2 + 0.13s + 0.24)}{(s - 0.003)(s + 6.77)(s^2 + 1.25s + 12.6)}$$

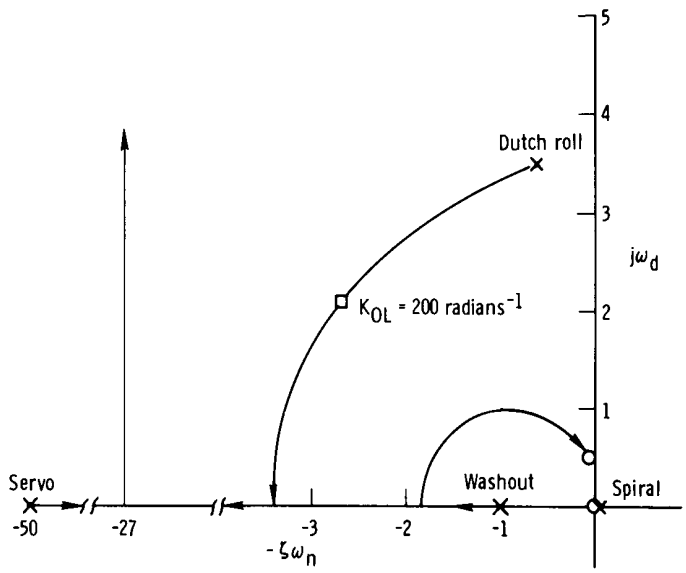

Figure 30. Root-locus diagram of yaw damper for cruise condition.

Another interesting result noted from the root-locus diagram is that the closed-loop Dutch roll damping is very dependent on the value of the washout time constant used in the feedback circuit. Slower time-constant values result in increased Dutch roll damping but reduce the rate at which the rudder returns to center after the yaw rate has reached a constant value during a turn maneuver. This results in increased sideslip and poor turn coordination, as seen by the pilot. Conversely, faster values of washout time constant improve turn coordination but greatly reduce the Dutch roll damping, thus canceling the effect of the damper. A washout time constant of 1 second was selected as a compromise between the two tradeoffs.

APPENDIX A

Turn Coordination

Turn coordination is achieved when the total sideslip of the airplane is zero during a steady turn maneuver. This results in the following relationship for coordination:

$$\beta_{total} = \frac{\beta}{\delta_r}(s)\delta_r + \frac{\beta}{\delta_a}(s)\delta_a = 0$$

Rearranging the right side of this expression, the relationship between aileron and rudder deflection for a coordinated turn can be expressed as

$$\frac{\delta_r}{\delta_a} = -\frac{\frac{\beta}{\delta_a}(s)}{\frac{\beta}{\delta_r}(s)}$$

This ratio can be expressed as the ratio of the numerator of $\frac{\beta}{\delta_a}(s)$ and $\frac{\beta}{\delta_r}(s)$ transfer functions, since both transfer functions have the same denominator. This gives the expression

$$\frac{\delta_r}{\delta_a} = \frac{\text{Numerator } \frac{\beta}{\delta_a}(s)}{\text{Numerator } \frac{\beta}{\delta_r}(s)}$$

Substituting the derived transfer functions (appendix B) for the landing-approach configuration results in the following relationship between aileron and rudder for a coordinated turn:

$$\frac{\delta_r}{\delta_a}(s) = \frac{0.158(s + 0.18)(s + 27)}{0.025(s - 0.11)(s + 3.80)(s + 80.3)}$$

It was shown in reference 7 that a good approximation for this rather complex expression can be achieved by using a first-order time lag with the corner frequency at 3.8 radians/sec. The expression can then be written as

$$\frac{\delta_r}{\delta_a}(s) \approx \frac{0.55}{\frac{s}{3.8} + 1}$$

The approximation is good for aileron frequencies between 0.5 radian/sec and 10 radians/sec.

The preceding relationship implies that turn coordination can be achieved relatively simply by filtering a signal proportional to aileron position and applying it to

the rudder. This technique was used in conjunction with the yaw damper. Aileron position was sensed with a potentiometer and applied to the rudder servoactuator through a first-order filter. This configuration provided adequate turn coordination over the entire flight envelope.

APPENDIX B

EQUATIONS OF MOTION AND AIRPLANE TRANSFER FUNCTIONS

LINEARIZED LATERAL-DIRECTIONAL EQUATIONS (BODY AXIS)

Side Force

$$\dot{\beta} = Y_\beta \beta + Y_p p + \frac{g}{V}\varphi - r + Y_r r + Y_{\delta_r}\delta_r$$

Rolling Moment

$$\dot{p} = L_\beta \beta + L_p p + L_r r + L_{\delta_a}\delta_a$$

Yawing Moment

$$\dot{r} = N_\beta \beta + N_p p + N_r r + N_{\delta_a}\delta_a + N_{\delta_r}\delta_r$$

AIRCRAFT TRANSFER FUNCTIONS

Cruise Condition

$$\frac{r}{\delta_r}(s) = \frac{-7.95(s + 6.72)\left[s^2 + 2(0.133)(0.495)s + (0.495)^2\right]}{(s - 0.003)(s + 6.77)(s^2 + 2(0.18)(3.55)s + (3.55)^2)}$$

$$\frac{\beta}{\delta_a}(s) = \frac{-0.737(s + 0.09)(s + 27.44)}{(s - 0.003)(s + 6.77)\left[s^2 + 2(0.18)(3.55)s + (3.55)^2\right]}$$

$$\frac{\beta}{\delta_r}(s) = \frac{0.043(s - 0.03)(s + 6.7)(s + 184.1)}{(s - 0.003)(s + 6.77)\left[s^2 + 2(0.18)(3.55)s + (3.55)^2\right]}$$

Landing-Approach Condition

$$\frac{r}{\delta_r}(s) = \frac{-1.96(s + 3.75)\left[s^2 + 2(0.04)(0.51)s + (0.51)^2\right]}{(s - 0.04)(s + 3.66)\left[s^2 + 2(0.2)(2.1)s + (2.1)^2\right]}$$

$$\frac{\beta}{\delta_a}(s) = \frac{-0.16(s + 0.18)(s + 27)}{(s - 0.04)(s + 3.66)\left[s^2 + 2(0.2)(2.1)s + (2.1)^2\right]}$$

$$\frac{\beta}{\delta_r}(s) = \frac{0.024(s - 0.11)(s + 3.81)(s + 80.3)}{(s - 0.04)(s + 3.66)\left[s^2 + 2(0.2)(2.1)s + (2.1)^2\right]}$$

APPENDIX C

POWER-SPECTRAL-DENSITY ANALYSIS

GENERAL TECHNIQUE

The power-spectral-density plots of airplane motions in turbulence presented in this report were obtained by using a spectral dynamics SD101A dynamic analyzer. The SD101A is a frequency-tuned bandpass filter which uses analog techniques for PSD analysis. The low-frequency cutoff of this instrument is 2 cps; thus, it was necessary to carry out the data processing in modified time, since the airplane's short-period frequencies were in the region of 0.3 cps to 0.5 cps. The technique used is discussed in detail in reference 8. It consisted of recording the real-time data on magnetic tape at a reel speed of 1 7/8 IPS and processing the data at a speed of 60 IPS. The effective frequency is then given by the expression

$$f_e = f\frac{S_R}{S_P} = f\left(\frac{1}{32}\right)$$

By using this modified time process, the lower limit of the analyzer was effectively reduced to 0.0625 cps. The power-spectral-density analysis was therefore restricted to frequencies between 0.0625 cps and 1.0 cps.

Bandwidth of Filter

Reference 9 points out that, as a practical compromise, the analyzer filter bandwidth should not be greater than one-fourth the width of the narrowest resonance expected to be encountered in the subject data. On the basis of this criterion, a real-time analyzer bandwidth of 2 cps was chosen, and the effective bandwidth, as a result of the modified time processing technique, is given by the expression

$$B = B_s\left(\frac{1}{32}\right) = \frac{2 \text{ cps}}{32} = 0.0625 \text{ cps}$$

Under this condition the statistical accuracy of the power-spectral-density plots will be approximately proportional to the filter bandwidth, as long as the resonance bandwidth of the data is greater than 0.25 cps at the half-power point.

Length of the Sample

In analyzing random analog data, for a constant analyzer filter bandwidth the statistical accuracy is controlled by the tape length and is given by the expression (ref. 10)

$$n = 2BT$$

where T is the data-tape length in seconds and n is the number of degrees of freedom

incorporated in the processing and is directly related to the statistical accuracy. In order to preserve n, it was desired to make the data tape as long as possible. The maximum tape length acceptable by the processing unit used with the SD101A was 72 feet. Selecting a maximum tape length would result in a real-time data sample of 7.7 minutes.

Because of the relatively long sample time required, it was necessary to carefully select a satisfactory level not only of turbulence intensity but also of duration. Previous experimental results (ref. 11) showed that, as a rule, most turbulence can be assumed to be homogeneous and stationary for a time duration of about 5 minutes. This was found to vary somewhat, however, with the type of turbulence (clean air, cumulus clouds, for example) and with the spatial region of the disturbance. For the random data analysis discussed and presented in this report, all turbulence was considered to be both homogeneous and stationary.

Averaging Time

An optimum averaging time was taken to be one-half the data-tape length in seconds (ref. 10). Since the maximum data-tape length in modified time (60 IPS) was approximately 14 seconds, an averaging time of 7 seconds was used.

Sweep Rate

In using an analog power-spectral-density analyzer, the frequency spectrum must be swept slow enough to allow the analyzer filter and averaging time constant to respond properly. Reference 10 states that the sweep rate must be selected so that the energy within the filter can be sampled for $4T_A$ seconds, where T_A is the averaging time. Thus

$$\text{Sweep rate} = \frac{B}{4T} = 0.07 \text{ cps/sec}$$

Statistical Accuracy

The number of statistical degrees of freedom n is related to the number of samples per second and the duration of the samples, for a given random process. The higher n becomes, the more accurate (in a statistical sense) any given power-density measurement becomes. In this report, the value of n for each power-spectral-density plot is specified.

APPENDIX D

SUMMARY OF EVALUATION PILOTS' GENERAL COMMENTS

PILOT 1

The yaw damper with interconnect provides a significant improvement in the handling qualities of the test airplane during a low-speed ILS approach in turbulence. Whether it would be better for a private aircraft owner with a $1000 budget to buy a yaw-damper system instead of some other equipment (a backup NAV/COM system, for example) is a question which would depend on many other factors.

PILOT 2

After several practice runs, my last two ILS approaches seemed easy, both with and without the yaw damper. However, I felt the yaw damper would help reduce the chances of serious deviation from the localizer if the pilot's attention were diverted.

PILOT 3

No comment.

PILOT 4

The effect of the system is a definite reduction in the pilot workload for all tasks. In addition, there is a slight improvement in vehicle response to turbulence.

Perhaps some pilots can adapt to the feet-on-the-floor technique during ILS approaches; however, I felt more comfortable with my feet on the pedals, and I believe my performance was better. I did not attempt an ILS approach using rudder inputs and systems ON because I believe the rudder control pressures would cancel some of the effects of the damper.

I believe that such a system as this, plus having the capability to "sum" the rudder control inputs from the pilot, would result in an uncontested and significant improvement in the handling qualities of the airplane.

PILOT 5

No comment.

APPENDIX D

PILOT 6

It's easiest to say unequivocally what the system does not do. It does not make an ILS approach in turbulent conditions dramatically easier. It provides several small improvements in ease and precision, and possibly safety, and some improvement in ride qualities.

PILOT 7

The yaw damper improves the overall lateral-directional characteristics of the test airplane in the cruise and approach configurations. The most improvement noted was in cruise conditions in turbulent air. The yaw damper improved the approach configuration, but did not seem to remove all unwanted yaw.

The feedback to the rudder pedals is undesirable and would not be a desired feature in a production system.

PILOT 8

No comment.

PILOT 9

The heading control task without the yaw damper required maximum pilot concentration to do a satisfactory job. With yaw damping and turn coordination, a considerable reduction in workload in order to accomplish satisfactory heading control is noticed.

PILOT 10

No comment.

PILOT 11

ILS approach with damper off required almost constant monitoring of heading and/or bank angle. Even the light turbulence caused the heading to change approximately 5° to 10° without any motion cues. With the damper on, it was much easier to control heading, but bank angle still varied quite easily.

APPENDIX D

PILOT 12

I saw no reduction in overall workload as a result of yaw damper and turn coordinator. The yawing oscillations can be ignored during an ILS approach in this airplane under these conditions, and the task can still be accomplished.

PILOT 13

Yaw damper helped.

PILOT 14

The yaw-rate damper improved the handling characteristics of the airplane during all maneuvers. Residual yaw oscillations following aileron inputs were almost nonexistent, permitting the airplane to be comfortably flown without using the rudder pedals. In mild turbulence, both ride and control were improved. The effects of asymmetric power resulting from poor throttle coordination during power changes were nearly eliminated. Landing approaches were much easier, with considerably less tendency to overcontrol.

The yaw-rate damper with the aileron-to-rudder interconnect produced still better handling characteristics. With this system operating, the airplane felt and handled like a much larger, heavier, and higher-wing-loaded airplane—very solid. The airplane was easily and precisely controlled without the use of the rudder pedals, except during flare and touchdown. Rudder-pedal action was of no concern; in fact, it was a comforting indication that the system was still with you.

PILOT 15

Even though my pilot rating for ILS approaches is the same with and without the damper, there was noticeable improvement in handling with the use of the damper. The ratings remained the same because of other airplane characteristics.

REFERENCES

1. Barber, Marvin R.; Jones, Charles K.; Sisk, Thomas R.; and Haise, Fred W.: An Evaluation of the Handling Qualities of Seven General-Aviation Aircraft. NASA TN D-3726, 1966.

2. Ellis, David R.; and Seckel, Edward: Flying Qualities of Small General Aviation Airplanes. Part 1: The Influence of Dutch-Roll Frequency, Dutch-Roll Damping, and Dihedral Effect. Rep. No. DS-69-8, FAA, June 1969.

3. Jones, J. G.: Simplified Spectral Analysis of the Motion of an Aircraft With a Saturating Yaw-Damper. Tech Rep. No. 65100, Brit. R.A.E., May 1965.

4. Dobrolenskii, Yu. P. (J. W. Palmer, trans.): The Effect of an Autopilot on the Dynamics and Flight Safety of a Non-Rigid Aircraft in a Turbulent Atmosphere. Lib. Trans. No. 1096, Brit. R.A.E., Jan. 1965.

5. Anon.: Flying Qualities of Piloted Airplanes. Military Specification MIL-F-8785B (ASG), Aug. 7, 1969.

6. Fink, Marvin P.; and Freeman, Delma C., Jr.: Full-Scale Wind-Tunnel Investigation of Static Longitudinal and Lateral Characteristics of a Light Twin-Engine Airplane. NASA TN D-4983, 1969.

7. Blakelock, John H.: Automatic Control of Aircraft and Missiles. John Wiley & Sons, Inc., c. 1965.

8. Morrow, Charles T.: Averaging Time and Data-Reduction Time for Random Vibration Spectra. I. J. Acoust. Soc. Am., vol. 30, no. 5, May 1958, pp. 456-461.

9. Bendat, Julius S.; Enochson, Loren D.; Klein, G. Harold; and Piersol, Allan G.: The Application of Statistics to the Flight Vehicle Vibration Problem. ASD Tech. Rep. No. 61-123, U.S. Air Force, Dec. 1961.

10. Bendat, Julius S.; and Piersol, Allan G.: Measurement and Analysis of Random Data. John Wiley & Sons, Inc., c. 1966.

11. Houbolt, John C.; Steiner, Roy; and Pratt, Kermit G.: Dynamic Response of Airplanes to Atmospheric Turbulence Including Flight Data on Input and Response. NASA TR R-199, 1964.

TABLE 1. – PHYSICAL CHARACTERISTICS OF TEST AIRPLANE

Length, ft	25.16
Height, ft	8.24
Mass, slugs	100
Wing –	
Incidence, deg	2
Dihedral, leading edge, deg	5
Wing chord, ft	5
Wing span, ft	35.98
Area, including aileron and flaps, ft^2	178
Length of flap, each, in.	110.9
Length of aileron, each, in.	75.3
Total aileron area, ft^2	14.1
Total flap area, ft^2	20.2
Stabilator –	
Overall span, ft	12.5
Total area, ft^2	32.5
Mean chord, ft	2.7
Vertical tail –	
Fin area, ft^2	9
Rudder area, ft^2	5.2
Rudder mean aerodynamic chord, ft^2	1.2
Moments of inertia, slug-ft^2 –	
I_X	2515
I_Y	1825
I_Z	4225

TABLE 2. – PILOT RATING SCALE

General classification	Numerical rating	Handling Qualities	Ability to complete mission	Ability to land
Satisfactory	1	Easy to control precisely; little corrective control required.	Yes	Yes
	2	Good response but necessitates attention for precise control.	Yes	Yes
	3	Acceptable controllability, but more than desired attention generally needed.	Yes	Yes
Unsatisfactory	4	Submarginal for normal use; requires excessive pilot attention.	Yes	Yes
	5	Controllability poor; demands constant pilot attention and continuous control inputs.	Probably	Yes
	6	Can be controlled, but pilot must exercise considerable care.	Doubtful	Yes
Unacceptable	7	Difficult to control and demands considerable pilot concentration.	No	Probably
	8	Controllable only with a high degree of pilot concentration and large control inputs.	No	Doubtful
	9	Extremely dangerous; can be controlled only with exceptional piloting skill.	No	No
	10	Uncontrollable.	No	No

Table 3. – SUMMARY OF PILOT BACKGROUND AND EXPERIENCE

Pilot	Background	Total time, hr	General-aviation time, hr
1	General aviation	4,000	4,000
2	General aviation	11,000	11,000
3	General aviation	500	500
4	Airlines and general aviation	11,000	2,000
5	Military and general aviation	3,800	2,200
6	Test pilot	3,000	200
7	Test pilot	5,000	700
8	Test pilot	4,800	2,500
9	Test pilot	4,800	500
10	Test pilot	4,700	600
11	Test pilot	5,500	1,000
12	Test pilot	4,800	500
13	Test pilot	5,000	500
14	Military	1,500	100
15	Military	2,000	700

TABLE 4. – RIDE-QUALITY RATING SCALE

Rating	Adjective	Characteristic qualities	Seat belts
Acceptable	1 Pleasant 2 Mildly unpleasant 3 Unpleasant	Calm air, smooth ride. Motion noticeable, generally comfortable. Side-to-side motion apparent, some discomfort, slight strain against belts.	Not required
Unsatisfactory	4 Distracting 5 Annoying 6 Objectionable	Motion generally uncomfortable, distracts reading, difficult to write. Definite strain against seat belt, writing very difficult. Writing impossible, increased tension.	Advisable and recommended
Unacceptable	7 Disturbing 8 Very disturbing 9 Alarming	Impossible to read, pressed hard against seat belt. Thrown violently against seat belt, possible injury. Objects flying in cabin, minor injury.	Mandatory
Catastrophic	10 Very alarming	Major injury.	----------

TABLE 5. – LATERAL-DIRECTIONAL STABILITY DERIVATIVES OF THE TEST AIRPLANE

Derivative	Approach	Cruise
Y_β, sec^{-1}	-0.1750	-0.2435
Y_p, $radians^{-1}$	-.00753	-.002887
Y_r, $radians^{-1}$	.00923	.00727
Y_{δ_r}, sec^{-1}	.02446	.04313
L_β, sec^{-2}	-4.144	-16.05
L_p, sec^{-1}	-3.666	-6.67
L_r, sec^{-1}	1.870	1.906
L_{δ_a}, sec^{-2}	-4.604	-18.05
N_β, sec^{-2}	3.323	10.52
N_p, sec^{-1}	-.558	-.738
N_r, sec^{-1}	-.8043	-1.104
N_{δ_a}, sec^{-2}	.195	.795
N_{δ_r}, sec^{-2}	-1.963	-7.95

NASA-Langley, 1970 — 2 H-584